Living Reviews in Solar Physics (2023) 20:3
https://doi.org/10.1007/s41116-023-00037-y

REVIEW ARTICLE

Models for the long-term variations of solar activity

Bidya Binay Karak[1]

Received: 8 October 2022 / Accepted: 26 May 2023 / Published online: 26 June 2023

Abstract

One obvious feature of the solar cycle is its variation from one cycle to another. In this article, we review the dynamo models for the long-term variations of the solar cycle. By long-term variations, we mean the cycle modulations beyond the 11-year periodicity and these include, the Gnevyshev–Ohl/Even–Odd rule, grand minima, grand maxima, Gleissberg cycle, and Suess cycles. After a brief review of the observed data, we present the dynamo models for the solar cycle. By carefully analyzing the dynamo models and the observed data, we identify the following broad causes for the modulation: (1) magnetic feedback on the flow, (2) stochastic forcing, and (3) time delays in various processes of the dynamo. To demonstrate each of these causes, we present the results from some illustrative models for the cycle modulations and discuss their strengths and weakness. We also discuss a few critical issues and their current trends. The article ends with a discussion of our current state of ignorance about comparing detailed features of the magnetic cycle and the large-scale velocity from the dynamo models with robust observations.

Keywords Solar physics · Solar activity · Solar cycle · Solar dynamo

Contents

✉ Bidya Binay Karak
karak.phy@iitbhu.ac.in

[1] Department of Physics, Indian Institute of Technology (Banaras Hindu University), Varanasi 221005, India

1 Introduction

The most prominent and fundamental feature of the solar magnetic field is its 11-year cyclic oscillation. Systematic observations of the large-scale solar magnetic field, available since the 1950 s, revealed the reversals of the field. However, the times of the reversals and the strength of the field are not the same for all the cycles. Time series of sunspot number and the sunspot area, for which we have direct observations for longer durations (group sunspot number since 1610 and the area since 1874), also show cycle-to-cycle variations (Hathaway 2015); Fig. 1. Thus, there is no doubt that the 11-year solar cycle is not regular and that makes the prediction of the future cycle a formidable task (Petrovay 2020). The prediction, however, is essential as the Sun's magnetic field drives the space weather which sometimes poses serious problems to us—e.g., by damaging satellite's electronics, modern-day technologies such as telecommunications, GPS networks, and electric power grids at high latitudes, making polar routes dangerous for aviation, increasing the radiation dose to astronauts in space (Temmer 2021). Evidence suggests that the variable solar

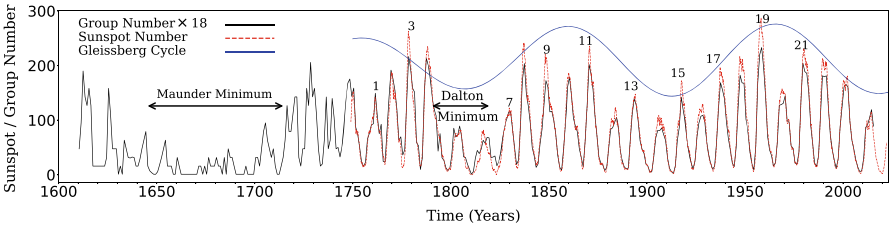

Fig. 1 Yearly variation of the monthly mean sunspot number smoothed using a Gaussian filter of FWHM = 7 months (red curve), available since 1749 and the yearly mean group sunspot number (black curve) available during 1610–2015. Note that group number is scaled by a factor of 18 to bring it to the scale of sunspot number. The blue curve with 98-year period guides the Gleissberg cycle. Cycle numbers for which the Even–Odd effect is obeyed are shown by tagging the number on the odd cycles. Data source: WDC-SILSO, Royal Observatory of Belgium, Brussels

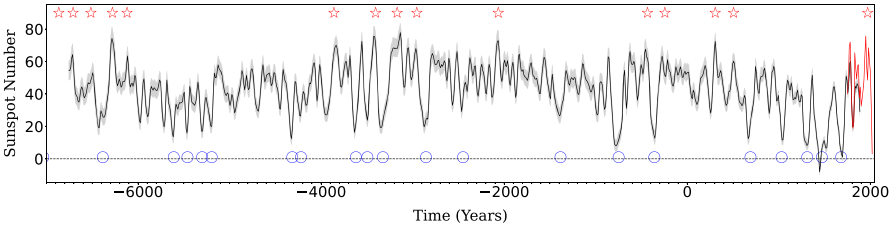

Fig. 2 Reconstructed (decadal) sunspot number along with its 68% confidence interval (gray shading) over nine millennia derived from ^{14}C data using a multi-proxy Bayesian method by Wu et al. (2018). The red curve shows the decadally resampled international sunspot number for the last 300 years (version 2, scaled by 0.6). The dashed line marks the zero spot number. Asterisks and circles mark the times of occurrences of grand maxima and minima, respectively

activity may also drive changes in the Earth's global temperature (Solanki et al. 2013).

Simply saying that the solar cycle is irregular is not enough to describe its true nature; there are many distinct features—such as grand minima and grand maxima—which can be considered as extreme examples of irregularity; Fig. 2. Additionally, there are some long-term patterns beyond the usual 11-year variation, such as Gnevyshev–Ohl rule and Gleissberg cycle. Below we briefly discuss these long-term variations. However, the readers can check the excellent reviews (Hathaway 2015; Usoskin 2023; Biswas et al. 2023) for extensive discussion.

2 Long-term variations of the solar cycle

2.1 Grand minima and maxima

Grand minima are the extended episodes of considerably lower magnetic activity than the normal one. The best example of these is the Maunder minimum in the 17th century when solar activity was considerably weaker than the normal one for about 70 years (Eddy 1976); Fig. 1. We emphasize that this is not an artifact due to few

observations but a real and well-observed event (Hoyt and Schatten 1996). Observations have shown that the Maunder minimum was not complete lack of activity—the Sun was still producing spots and even cycles but at a lower rate (Beer et al. 1998; Zolotova and Ponyavin 2015; Usoskin et al. 2015; Vaquero et al. 2015; Zolotova and Ponyavin 2016. This makes the Maunder minimum (and possibly all grand minima) a special state of solar activity. Further distinct aspects of Maunder minimum are the followings. (1) There was a strong hemispheric asymmetry during the latter half of Maunder minimum; sunspots were observed mostly in the southern hemisphere (Ribes and Nesme-Ribes 1993). (2) Recovery of Maunder minimum is gradual, however, the onset is somewhat uncertain (Fig. 1). Some previous results suggested that the onset is abrupt (Usoskin et al. 2000), while later studies showed that it is likely to be gradual (Vaquero et al. 2011). (3) A proxy of solar activity inferred from a cosmogenic isotope ^{14}C showed that the cycle length before the onset of the Maunder minimum was significantly longer than its usual value (Miyahara et al. 2021; Usoskin et al. 2021).

Analyses of ^{14}C for the last 11,400 years revealed the following important results (Usoskin et al. 2007; Usoskin 2023; Usoskin et al. 2021). (1) The Sun spent about 17% of its time in the grand minimum state. (2) Grand minima are of two types: short minima of Maunder type with duration 30–90 years and long ($>$ 100 years) minima of Spörer type. (3) The grand minima recur aperiodically. (4) The waiting time distribution of the occurrence of grand minima displays a deviation from an exponential distribution. However, Moss et al. (2008) showed that feature (5) can be an artifact of poor statistics (it is based on only 27 grand minima identified in the observed data).

Grand maxima, on the other hand, are extended periods with appreciably higher magnetic activity than the normal one. The modern maximum that occurred around 1960 is an example of the same. In about last 11,000 years, 23 grand maxima were detected and the Sun spent about 12% of its time in this phase (Usoskin et al. 2007; Usoskin 2023). Grand maxima are more short-lived than the grand minima (Solanki et al. 2004; Usoskin et al. 2021). The distribution of the duration of grand maxima shows a smooth variation with an exponential fall at longer durations. The distribution of the waiting time between the consecutive grand maxima is not conclusive but there is an indication of deviation from the exponential law.

2.2 Cycles and modulations beyond 11 years

Beyond the regular 11-year solar cycle, the following longer cycles or modulations are detected in the solar activity data.

- Gnevyshev–Ohl rule/Even–Odd effect: This says that if the cycles are arranged in pairs with the even cycle and the following odd cycle, then the sum of the sunspot number in the odd cycle is higher than the even cycle (Gnevyshev and Ohl 1948). We note that this is not a strict rule, it is violated in cycle pairs: 4–5, and 22–23 (Hathaway 2015).

- Gleissberg cycle: a modulation in the solar activity with a mean period of about 90 years (Gleissberg 1939; Hathaway 2015). Recent data shows that a sinusoidal fit to the detrended amplitude gives an approximate period of 98 years as shown in Fig. 1; also see Forgács-Dajka et al. (2004) who found somewhat closer value (104 years) in the area-weighted sunspot group data.
- Suess/de Vries cycle: Cycle with a period of 205–210 years detected in the cosmogenic isotopes (Suess 1980).

Some other cycles like the millennial Eddy cycle and 2400-year Hallstatt cycle are also noticed in the cosmogenic isotope, however, their signals are poor and require longer data to confirm (Usoskin 2023).

We would like to mention that not only the solar cycle is irregular, but the magnetic cycles that are observed in other sun-like stars are also irregular (Boro Saikia et al. 2018; Garg et al. 2019). Analyzing the data of 111 stars of spectral type F2–M2, Baliunas et al. (1995) showed that the slowly rotating (old) stars show a smoother variability in the magnetic cycle and possibly occasional grand minima, whereas the rapidly rotating young stars show irregular activity and no grand minima. Recently, Shah et al. (2018) and Baum et al. (2022) claim that HD 4915 and HD 166620 are possibly entering into the grand minimum phase. Hence, stellar cycles are also interesting in terms of their modulations.

Now we shall come to the models for these long-term variations of solar activity. By models in this article, we mean the dynamo models that are used to explain the long-term variations of solar activity. Below we first present an introductory discussion of the solar dynamo (Sect. 3) and models (Sect. 4). Then we identify the causes of the long-term modulations (Sect. 5), followed by some illustrative models for the same (Sects. 6 and 7). Finally, we discuss a few open questions with current trends (Sect. 8) and end the article with concluding remarks (Sect. 9).

3 Solar dynamo: an overview

Dynamo is a process in which a sufficiently strong and complex plasma flow maintains a magnetic field by overcoming its Ohmic dissipation. The magnetic fields that give rise to sunspots, global dipole magnetic field, and 11-year cycle are essentially of the large-scale (global) type which usually requires a non-zero net helicity (mirror asymmetry) in the flow. Due to the global rotation, the convective motion of plasma in the Sun is helical and the rotation is differential (nonuniform). Through this helical flow, the poloidal field in the Sun is primarily generated from the toroidal field, while the poloidal field acts as a source for the toroidal field through the differential rotation (Parker 1955a). Thus, the solar dynamo is essentially a cyclic oscillation between two fields and the turbulent transport plays an essential role in this oscillation (Sect. 4). For a detailed discussion of the solar dynamo, we refer the readers to the comprehensive reviews by Ossendrijver (2003) and Charbonneau (2020).

To study the solar dynamo, we need to begin with at least two basic equations of the magnetohydrodynamics, namely,

$$\frac{\partial \boldsymbol{B}}{\partial t} = \boldsymbol{\nabla} \times (\boldsymbol{v} \times \boldsymbol{B} - \eta \boldsymbol{\nabla} \times \boldsymbol{B}), \tag{1}$$

$$\rho \left[\frac{\partial \boldsymbol{v}}{\partial t} + (\boldsymbol{v} \cdot \boldsymbol{\nabla}) \boldsymbol{v} \right] = - \boldsymbol{\nabla} P + \boldsymbol{J} \times \boldsymbol{B} + \boldsymbol{\nabla} \cdot (2 \nu \rho \boldsymbol{S}) + \boldsymbol{F}, \tag{2}$$

where $\boldsymbol{B}$ and $\boldsymbol{v}$ are the magnetic and velocity fields, respectively, η is the magnetic diffusivity, ρ is the density, P is the pressure, $\boldsymbol{J} = \boldsymbol{\nabla} \times \boldsymbol{B}/\mu_0$, the current density, ν is the kinematic viscosity, $S_{ij} = \frac{1}{2}(\nabla_i v_j + \nabla_j v_i) - \frac{1}{3}\delta_{ij} \boldsymbol{\nabla} \cdot \boldsymbol{v}$ is the rate-of-strain tensor and the term $\boldsymbol{F}$ includes gravitational, Coriolis and any other body forces acting on the fluid.

The above equations must be solved along with the mass continuity, internal energy and equation of state in the solar CZ with appropriate boundary conditions. This approach to studying the solar dynamo—so-called global MHD simulations—was pioneered by Gilman (1983) and Glatzmaier (1984) in the 1980 s. While these simulations gave a few positive results (e.g., large-scale flows and field and a bit of polarity reversal), being computationally expensive, these simulations were hardly applied to explore the long-term variations of the solar cycle. Further, the applicability of these simulations in the Sun is questionable due to their operation in a completely different parameter regime. In recent years, however, we have got some encouraging results in the global MHD simulations, a few of them were run for several magnetic cycles to explore the cycle modulations. In Sect. 7, we shall discuss the modulations of cycles found in these simulations. Probably the biggest problem in these simulations is to explore and understand the cause of solar cycle variabilities. In fact, often an equivalent mean-field model is set up to identify dynamics of the magnetic field in these global MHD simulations. On the other hand, the mean-field models have been extensively employed in the past to explore the cause of solar cycle variability. Therefore, below we shall consult the mean-field version of the above equations to identify various mechanisms that can possibly lead to cycle modulations.

Writing the magnetic and velocity fields in terms of mean/large-scale and fluctuating/small-scale parts and applying suitable approximations in Eqs. (1) and (2), one can obtain the following equations (Krause and Rädler 1980).

$$\frac{\partial \overline{\boldsymbol{B}}}{\partial t} = \boldsymbol{\nabla} \times (\overline{\boldsymbol{v}} \times \overline{\boldsymbol{B}} + \overline{\mathcal{E}}), \tag{3}$$

$$\rho \left[\frac{\partial \overline{\boldsymbol{v}}}{\partial t} + (\overline{\boldsymbol{v}} \cdot \boldsymbol{\nabla}) \overline{\boldsymbol{v}} \right] = - \boldsymbol{\nabla} P + \overline{\boldsymbol{J}} \times \overline{\boldsymbol{B}} + \overline{\boldsymbol{J}' \times \boldsymbol{B}'} - \boldsymbol{\nabla} \cdot \rho \overline{\boldsymbol{Q}} + \overline{\boldsymbol{F}}, \tag{4}$$

where the quantities with overline and prime respectively denote the mean and fluctuating components. The mean electromotive force $\overline{\mathcal{E}}$ is given by

$$\overline{\mathcal{E}} = \overline{\boldsymbol{v}' \times \boldsymbol{B}'}. \tag{5}$$

In the mean-field theory, this $\overline{\mathcal{E}}$ is written in terms of the mean magnetic field in some

limiting case (which holds at small Strouhal and magnetic Reynolds numbers) as follows.

$$\overline{\mathcal{E}}_i = \hat{\alpha}_{ij}\overline{B}_j + \hat{\eta}_{ijk}\frac{\partial \overline{B}_j}{\partial x_k}, \tag{6}$$

Some components of $\hat{\alpha}$ tensor give the dynamo action and some of the components of $\hat{\eta}$ tensor are responsible for the diffusion of fields. For homogeneous and isotropic turbulence, one can show that

$$\overline{\mathcal{E}} = \alpha\overline{\boldsymbol{B}} - \eta_t(\boldsymbol{\nabla}\times\overline{\boldsymbol{B}}), \tag{7}$$

where $\alpha = -\frac{1}{3}\tau_{\rm corr}(\overline{\boldsymbol{v}'\cdot\boldsymbol{\nabla}\times\boldsymbol{v}'} - (\rho\mu_0)^{-1}\overline{\boldsymbol{B}'\cdot\boldsymbol{\nabla}\times\boldsymbol{B}'})$ and $\eta_t \approx \frac{1}{3}\tau_{\rm corr}\overline{\boldsymbol{v}'\cdot\boldsymbol{v}'}$. In the classical $\alpha\Omega$ dynamo model, this α coefficient is the one which is responsible for the generation of the poloidal magnetic field from the toroidal one (Parker 1955a; Steenbeck et al. 1966). The turbulent diffusivity η_t is several orders of magnitude larger than the molecular η and that is the reason we have dropped out the η term in Eq. (3).

If the turbulence is inhomogeneous, then there will be an additional term $\boldsymbol{\gamma}\times\overline{\boldsymbol{B}}$ in the above $\overline{\mathcal{E}}$. This $\boldsymbol{\gamma}$ is the magnetic pumping which is usually ignored in most of the kinematic mean-field dynamo models, but found to be important in the solar dynamo (e.g., Guerrero and de Gouveia Dal Pino 2008; Karak and Nandy 2012; Kitchatinov and Olemskoy 2012; Cameron et al. 2012; Karak and Cameron 2016; Karak and Miesch 2017) and has also been detected in global convection simulations (Racine et al. 2011; Augustson et al. 2015; Simard et al. 2016; Warnecke et al. 2018).

The value of Q in Eq. (4) can be written in terms of Reynolds and Maxwell stresses as

$$\overline{Q}_{ij} = \overline{v_i'v_j'} - (\rho\mu_0)^{-1}\overline{B_i'B_j'} = \overline{Q}^{\lambda}_{ij} - \mathcal{N}_{ijkl}\frac{\partial\overline{v}_k}{\partial x_l}, \tag{8}$$

where the tensor $\mathcal{N}$ gives the turbulent viscosity ν_t. While $\mathcal{N}$ is rotation dependent and has a complex form, it has two simple terms in the case of isotropic turbulence. Again like η_t, ν_t is usually much larger than the molecular viscosity (ν) and thus the latter is neglected in Eq. (4).

The term $\overline{Q}^{\lambda}_{ij}$ is called the Λ effect which drives angular momentum in the rotating CZ (Kippenhahn 1963; Rüdiger 1989; Kichatinov and Rüdiger 1993) to give rise to the differential rotation. While the second term in Eq. (8) tends to smooth out the nonuniformity in rotation, $\overline{Q}^{\lambda}_{ij}$ makes the rotation nonuniform.

4 Some historical developments of the dynamo models

4.1 Axisymmetric kinematic dynamo equations

Despite tremendous contribution to the field, the pioneering simulations of Gilman (1983) and Glatzmaier (1984, 1985) were discouraging for the dynamo modellers as

they failed to reproduce most of the basic features of the solar magnetic field. Due to this failure, the dynamo modellers paid more attention to the mean-field models to study the solar cycle. Motivated by the observed large-scale magnetic and velocity fields, the coronal structure, and to make calculations simple, historically the mean-field solar dynamo was mostly studied under the axisymmetric approximation. With this approximation, the large-scale magnetic field can be written as

$$\overline{\boldsymbol{B}}(r,\theta,t) = \boldsymbol{B}_{\rm p} + \boldsymbol{B}_{\rm t} = \boldsymbol{\nabla} \times \left[A(r,\theta,t)\hat{\boldsymbol{\phi}}\right] + B(r,\theta,t)\hat{\boldsymbol{\phi}}, \tag{9}$$

where $\boldsymbol{B}_{\rm p} = B_r(r,\theta,t)\hat{\boldsymbol{r}} + B_\theta(r,\theta,t)\hat{\boldsymbol{\theta}}$ is the poloidal component of the magnetic field and $\boldsymbol{B}_{\rm t} = B(r,\theta,t)\hat{\boldsymbol{\phi}}$ is the toroidal component. Similarly, the velocity can be written as

$$\overline{\boldsymbol{v}}(r,\theta) = \boldsymbol{v}_{\rm m}(r,\theta) + v_\phi(r,\theta)\hat{\boldsymbol{\phi}} = v_r(r,\theta)\hat{\boldsymbol{r}} + v_\theta(r,\theta)\hat{\boldsymbol{\theta}} + r\sin\theta\Omega(r,\theta)\hat{\boldsymbol{\phi}}, \tag{10}$$

where $\boldsymbol{v}_{\rm m} = v_r(r,\theta)\hat{\boldsymbol{r}} + v_\theta(r,\theta)\hat{\boldsymbol{\theta}}$ is the meridional circulation and $\Omega(r,\theta)$ is the angular frequency.

We note that here we have taken the velocity as the time-independent (steady), which is the case when we make the kinematic approximation. The kinematic approach has been adopted extensively in the literature to study the solar dynamo because in this case, we do not have to consider the equation for the flow (Eq. 4) and thus it makes the dynamo problem linear (see Eqs. 11, 12) below) and thus simpler. Nevertheless, observations provide us with the azimuthal flow in the whole CZ and the meridional flow in the near-surface layer. Given the fact that the differential rotation shows a little variation (in the form of torsional oscillation), one would expect that the kinematic approach is not a bad assumption for the sun.

After substituting the above forms of the fields in Eq. (3) and using the value of $\overline{\mathcal{E}}$ from Eq. (7) one can derive the following equations.

$$\frac{\partial A}{\partial t} + \frac{1}{s}(\boldsymbol{v_m}\cdot\boldsymbol{\nabla})(sA) = \eta_t\left(\nabla^2 - \frac{1}{s^2}\right)A + \alpha B, \tag{11}$$

$$\frac{\partial B}{\partial t} + \frac{1}{r}\left[\frac{\partial(rv_rB)}{\partial r} + \frac{\partial(v_\theta B)}{\partial\theta}\right] = \eta_t\left(\nabla^2 - \frac{1}{s^2}\right)B + s(\boldsymbol{B_p}\cdot\boldsymbol{\nabla})\Omega + \frac{1}{r}\frac{d\eta_t}{dr}\frac{\partial(rB)}{\partial r}, \tag{12}$$

where $s = r\sin\theta$ and η_t is assumed to depend only on r.

In the above equations, the second term involving $\boldsymbol{v_m}$ (or equivalently v_r, v_θ) corresponds to advection of poloidal field by meridional flow and the first terms on the RHS of both equations represent the diffusion. In Eq. (11), the term αB is the source for the poloidal magnetic field. We discuss more about it in the next section. The term $s(\boldsymbol{B_p}\cdot\boldsymbol{\nabla})\Omega$ in Eq. (12) is the source for the toroidal field, in which the nonuniformity of the rotation along the direction of poloidal field induces a toroidal field (the Ω effect). We note that while deriving above equations we have neglected a term $\hat{\boldsymbol{\phi}}\cdot[\boldsymbol{\nabla}\times(\alpha\boldsymbol{B_p})]$. This is also a source for the toroidal field through the α-effect. However, in Sun we believe that this term is negligible compared to the source due to differential rotation. The dynamo model constructed based on this

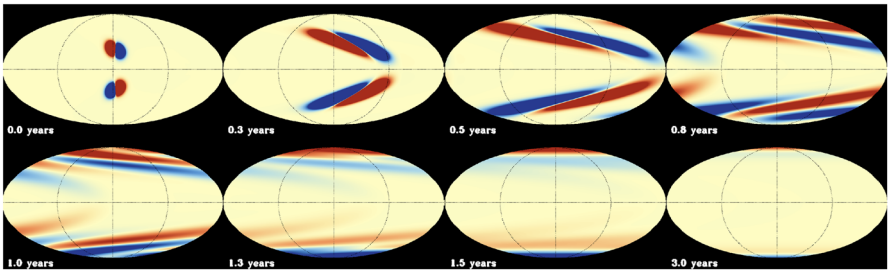

Fig. 3 Demonstration of Babcock–Leighton process. Decay and dispersal of two BMRs deposited symmetrically at 25° are shown for three years. Note that due to finite tilts ($\approx 14°$ as assigned by Joy's law) of the BMRs, a net poloidal field near the pole is produced (see the weak field near the pole in the last snapshot). Snapshots are taken from a 3D model (Karak and Miesch 2018) in which meridional flow (poleward on the surface), differential rotation (fast equator) and a turbulent diffusivity of 10^{12} cm^2 s^{-1}are specified. While the magnetic field in the initial BMR is 3000 G, it is saturated at 0.1 G to show the weak field at the end

assumption is traditionally called the $\alpha\Omega$ type dynamo in which the poloidal and toroidal fields maintain each other through a feedback loop. Finally, the last term in Eq. (12) gives rise to an advection due to nonuniform turbulent diffusion.

4.2 Babcock–Leighton dynamo models

There are two potential and widely studied mechanisms through which the poloidal field in the Sun can be generated. The first one was proposed by Parker (1955a) and mathematically studied in detail by Steenbeck et al. (1966). In this process, the helical convection (which has non-zero net helicity) in the CZ twists the toroidal field to generate a poloidal component. This is the traditional α-effect. We note that this process only operates when the energy density of the toroidal magnetic field is below the energy density of the convective turbulence so that the turbulent flow can twist the field. The second mechanism goes to Babcock (1961) and Leighton (1964) who proposed that the decay of tilted bipolar magnetic regions (BMRs) generates a poloidal field.

Observations show that the line joining the centres of poles of a BMR makes an angle with respect to the equatorial line. This tilt statistically increases with the latitude which is known as Joy's law (Hale et al. 1919). When a BMR decays, the magnetic field of two poles diffuses at slightly different latitudes. The field from the leading part predominantly cancels with the field from the other hemisphere across the equator and the trailing part is largely advected towards the pole to produce a global dipole moment for the Sun; see Fig. 3 and also see Hazra et al. (2017). This process of generating poloidal field, the so-called Babcock–Leighton process requires a tilt in the BMR and this process need not be very efficient in terms of the fact that the magnetic flux in the polar cap is approximately the net flux content in only one BMR ($\approx 5 \times 10^{21}$ Mx; Cameron and Schüssler 2015).

As the BMRs are produced from the deep-seated toroidal field and the decay of BMRs produces a poloidal field, this mechanism in many Babcock–Leighton type

dynamo models is phenomenologically prescribed by a term αB in Eq. (11). Here, α is nonzero only near the surface in contrast to the (classical) α-effect, which operates in the whole CZ. Although both the α-effect and Babcock–Leighton process for the generation of the poloidal field are captured by the same term αB in mean-field dynamo models, their mechanisms are completely different. Nevertheless, in some comprehensive dynamo models, e.g., the 3D model of Yeates and Muñoz-Jaramillo (2013), Miesch and Dikpati (2014), Kumar et al. (2019) and Bekki and Cameron (2022) and the 2×2D model of Lemerle and Charbonneau (2017), do not capture the Babcock–Leighton process through this αB term, instead, they include explicit BMRs which self-consistently generates the poloidal field. We further emphasise that the Babcock–Leighton dynamos are also of mean-field type although the Babcock–Leighton source term is often introduced in a heuristic way instead of strictly deriving it from the mean-field MHD.

There was little doubt, at least, after the helioseismology mapped the rotation profile in the CZ (Howe 2009) that the toroidal field in the Sun is produced through the Ω effect. However, it was not clear whether the helical α-effect or Babcock–Leighton process is the dominating mechanism for the generation of the poloidal field in the Sun. Most of the early dynamo models considered the α-effect. Then in the 1990 s, the studies from the thin flux tube model have shown that the tilt of the BMR is presumably produced due to the Coriolis force acting on the rising flux tube of the toroidal field in the CZ (D'Silva and Choudhuri 1993; Fan et al. 1994). These studies also showed that the magnetic field at the bottom of the CZ (BCZ) in the BMR forming regions[1] has to be of the order of 10^5 G, which is much higher than the equipartition field strength ($\sim 5 \times 10^3$ G; Stix 2002). If this is the case, then the classical α will not be able to operate in this strong field. However, the Babcock–Leighton process still can operate in this regime as in this process, the original toroidal field and the generated poloidal field are segregated in space and there is no generation of magnetic helicity and no catastrophic quenching (Kitchatinov and Olemskoy 2011a). This was a strong support behind the Babcock–Leighton process as the primary source for the poloidal field in the Sun.

We would like to recall that there are observational supports for the operation of the Babcock–Leighton process. First, there is a close connection between the locations of BMR emergences and the sites of the formations of the trailing polarity surges at low latitudes, as seen in the time-latitude distribution (or maybe in the Carrington maps) of the magnetic field (e.g., Mordvinov et al. 2020, 2022). Second, the Surface Flux Transport (SFT) models, which describe the evolution of the radial component of the magnetic field by utilizing the observed BMRs, large-scale flows (such as differential rotation and meridional circulation) and turbulent diffusion on the solar surface, capture the Babcock–Leighton process (Wang et al. 1989; Baumann et al. 2004; Upton and Hathaway 2014b; Jiang et al. 2014b). The remarkable success of the SFT model in terms of reproducing the observed magnetic field on the solar surface as well as the coronal structure gives support that at least the observed magnetic field in the Sun is largely due to the Babcock–Leighton process.

[1] During the BMR formation, the magnetic field may also be locally amplified from the diffuse field; see discussion in Getling and Buchnev (2019).

Next, the observed correlation between the polar field (or its proxy) at the end of the cycle and the amplitude of the next cycle (Wang and Sheeley 2009; Kitchatinov and Olemskoy 2011b; Muñoz-Jaramillo et al. 2013; Priyal et al. 2014; Kumar et al. 2021b, 2022) and the flux budgets of the observed and the generated poloidal and toroidal fields (Cameron and Schüssler 2015) suggest that the Babcock–Leighton process is possibly the main source of the poloidal field in the Sun.

4.3 Flux transport dynamo models

While developing a satisfactory dynamo model for the solar cycle in the Babcock–Leighton framework, modellers faced a challenge to reproduce the observed migration of sunspots. As the deep-seated toroidal field gives rise to sunspots and the latitudinal band of sunspots migrates towards the equator within a cycle, we expect the toroidal field in the deeper CZ to advect towards the equator with the progress of a cycle. However, to obtain an equatorward propagation through dynamo wave, Parker–Yoshimura sign rule demands that $\alpha \frac{\partial \Omega}{\partial r} < 0$ in the northern hemisphere (Parker 1955a; Yoshimura 1975). The observed profile of Ω shows that $\frac{\partial \Omega}{\partial r}$ is positive in the low latitudes where sunspots emerge. Furthermore, the observations of BMR tilts also suggest that the α corresponding to the Babcock–Leighton process is also positive in the northern hemisphere. Hence, Parker–Yoshimura sign rule suggests a poleward migration in contrast to observations. This problem was resolved by introducing a meridional flow such that it is equatorward in the deeper CZ. A sufficiently strong flow can overpower the poleward dynamo wave and can explain the equatorward migration of the sunspot belt (Wang et al. 1991; Choudhuri et al. 1995; Durney 1995; Hazra et al. 2014a). While the poleward component of the meridional flow on the surface has been well-known for many years, recent helioseismic observations find some indication of the equatorward (return) flow near the base of CZ (Rajaguru and Antia 2015; Gizon et al. 2020). Also, there is controversy about the depth of the return flow and the number of cells that exist in the CZ.

The dynamo models in which the equatorward migration of the toroidal field at the BCZ is driven by the meridional flow (or some other flow), rather than dynamo waves, are popularly known as the flux transport dynamo models (Wang et al. 1991; Choudhuri et al. 1995; Durney 1995); see Karak et al. (2014a) for a review on this topic. Usually, the Babcock–Leighton dynamo models (in which the poloidal source is due to the Babcock–Leighton process) include a meridional flow to produce the equatorward migration of the toroidal field and thus they are of flux transport type, however, an $\alpha\Omega$ type dynamo can also be of flux transport type if a sufficiently strong meridional flow is present. Usually, these flux transport dynamo models, consider a single cell (in each hemisphere) meridional circulation profile with a return flow of about a few meters per second at a depth of about $0.7\,R_{\odot}$. Most of the existing Babcock–Leighton type flux transport dynamo models are kinematic, however, see Rempel (2006), Inceoglu et al. (2017) and Bekki and Cameron (2022) for exceptions.

5 Mechanisms of long-term variations

With the above introduction to the solar dynamo theory, we shall explore how the irregular variations in the solar cycle can occur. Broadly, we can think of the following three major causes for these.

- Magnetic feedback on the flow
- Stochastic forcing
- Time delays in various processes of the dynamo

5.1 Magnetic feedback on the flow

We have seen in Sect. 3 that the flows are essential for the dynamo mechanism. The large-scale component of velocity, as appearing in Eq. (3), is observed in the form of differential rotation and meridional circulation in the Sun. The differential rotation induces a strong toroidal field from the poloidal one in the CZ. The meridional circulation transports the magnetic field near the surface from low to high latitudes where it pushes the field to the deeper CZ, and it possibly transports the field towards the equator near the BCZ. Hence, it is natural that any dynamical change in these large-scale flows can cause variation in the solar cycle.

In Eq. (4), we find several dynamical terms through which modulation in the flow can arise. First is the mean Lorentz force $\overline{\boldsymbol{J}} \times \overline{\boldsymbol{B}}$, which arises through the interaction between the mean magnetic and the mean current. This is also called the Malkus-Proctor effect (Malkus and Proctor 1975). The second is the small-scale feedback, which consists of two parts. One is the direct small-scale Lorentz forcing $\overline{\boldsymbol{J}' \times \boldsymbol{B}'}$ appearing in Eq. (4) (through the fluctuating current and magnetic field). Another is the dynamical modulation in the Λ effect, which comes from the anisotropic turbulence (appearing through $\overline{Q}$ in Eq. 8). This modulation arises because the mean magnetic field also gives rise to the Lorentz force on the small-scale turbulence (Kitchatinov et al. 1994b). This, so-called micro (small-scale) feedback, has been captured through a simple quenching in the Λ effect in many mean-field dynamo models (Küker et al. 1999). The dynamo-induced small-scale magnetic field also affects the large-scale flows and the turbulent transport; see Eqs. (4, 7, 8) and Käpylä (2019).

Next, the magnetic field gives feedback on the dynamo coefficients. The magnetic field dependence of the α coefficient is popularly studied in the literature (Pouquet et al. 1976; Field and Blackman 2002; Subramanian and Brandenburg 2004). While we do not have an analytical theory for the magnetic field dependence of the dynamo coefficients from the first principle, Rüdiger and Kichatinov (1993) and Kitchatinov et al. (1994a) respectively gave the dependences of the α and η on the magnetic field using the quasi-linear and quasi-isotropic turbulence. Based on this theory, when the magnetic field is much larger than the equipartition field strength, the α falls as $1/B^3$, while many kinematic dynamo models traditionally use a quenching factor $1/\left(1+(B/B_{\rm eq})^2\right)$ with $B_{\rm eq}$ being the equipartition field. MHD turbulent (Käpylä

and Brandenburg 2009; Karak et al. 2014b) and global convection simulations (Racine et al. 2011; Simard et al. 2016; Warnecke et al. 2018) also do show some magnetic quenching in α. Whatever be the exact magnetic field-dependent form of α, in all these results one thing is clear: as the magnetic field tries to grow, it suppresses α and this in turn reduces the generation of the magnetic field. Hence, the nonlinearity in α tries to make the cycle regular, rather than producing irregularity in the cycle, provided the strength of α is not much higher than the critical α.

The feedback on the small-scale turbulence can also be seen in the modulation of turbulent viscosity and magnetic diffusivity, which can in turn give some variation in the magnetic field. However, due to difficulties in computing these turbulent coefficients, we have limited knowledge on how much cycle modulation can arise due to magnetic feedback on the turbulent coefficients; anyhow, see the results of quasi-linear approximation (Kitchatinov et al. 1994a) and the convection simulations cited above. Unlike α quenching, the diffusivity quenching, however, tends to make the model unstable by increasing the magnetic field when the field strength is large (Kitchatinov and Olemskoy 2010) and thus unless some other mechanism, say α quenching is included, the dynamo usually does not produce stable cycle (Kitchatinov and Olemskoy 2010; Vashishth et al. 2021). The last two references have also shown that the nonlinearities in α and η produce dynamo hysteresis—strong oscillatory magnetic field in the subcritical regime if the dynamo is started with a strong field and decaying solution otherwise if started with a weak field. This was also confirmed in numerical simulations of turbulent dynamos (Karak et al. 2015b; Oliveira et al. 2021).

We would like to emphasize that the recent observations of stellar rotation (Metcalfe et al. 2016) show that the rate of solar rotation is close to the minimum rate for the onset of the large-scale dynamo (also see Rengarajan 1984). Furthermore, Cameron and Schüssler (2017) and Cameron and Schüssler (2019) showed that the variability seen in the cosmogenic isotope for the last 10,000 years is consistent with the results from the generic normal form model for a noisy and weakly nonlinear limit cycle. Grand minima are only produced when the dynamo is not highly supercritical and the Sun and solar-like slowly rotating stars do produce grand minima (Kitchatinov and Olemskoy 2010; Kumar et al. 2021a; Vashishth et al. 2021, 2023). All these suggest that the solar dynamo is only slightly supercritical and weakly nonlinear. Thus, possibly the nonlinear effects are not very important in producing long-term modulations in the solar cycle.

5.2 Stochastic forcing

Solar CZ is highly turbulent and the turbulent quantities (appearing in Eqs. (7) and (8)) are subjected to fluctuations around their means in a time scale equal to the correlation time of the turbulent convection. As there is a finite number of convection cells over the longitudes at a given latitude in the Sun, the fluctuations in the turbulent coefficients are significant compared to their mean values. Hoyng (1988) argued that the fluctuations in the α-effect can be larger than its mean and thus they can produce variation in the solar cycle (Choudhuri 1992; Hoyng 1993; Ossendrijver et al. 1996). In fact, due to small-scale dynamo, there are always fluctuations around

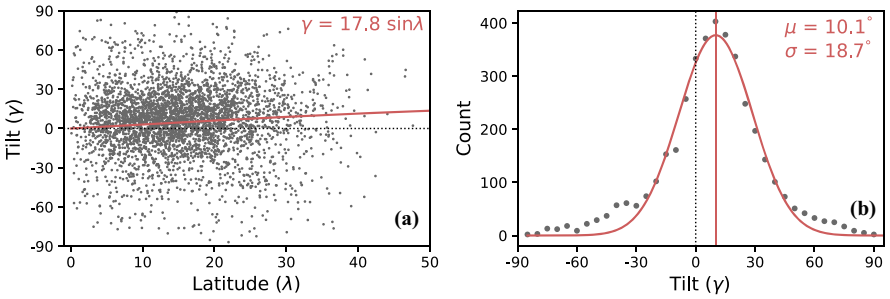

Fig. 4 Tilt angles of BMRs computed by "tracking" the MDI line-of-sight magnetograms covering the Cycle 23 (1996 September–2008 December). Here each BMRs are tracked over their lifetimes and the tilt and latitude of a BMR are taken by averaging their values over its time evolution when the flux is more than 60% of its maximum. In **a** solid line guides Joy's law: $\gamma = 17.8 \sin\lambda$. **b** Shows the tilt distribution (with 5° bin size) with fitted Gaussian (solid line) of $\mu = 10.1°$ and $\sigma = 18.7°$. The figure is produced using the data presented in Sreedevi et al. (2023)

$\overline{\mathcal{E}}$ (Brandenburg et al. 2008; Brandenburg and Spiegel 2008). The fluctuations in the angular momentum transport (as parameterized by the Λ effect; Eq. 8) can also alter the differential rotation and meridional circulation and thus can produce modulations in the solar cycle (Rempel 2005; Inceoglu et al. 2017).

Babcock–Leighton process, in which decay and dispersal of tilted BMRs generate a poloidal field in the Sun, involves some intrinsic fluctuations. The tilts of BMRs have a considerable amount of scatter around Joy's law (Howard 1991; Stenflo and Kosovichev 2012; McClintock et al. 2014; Senthamizh Pavai et al. 2015; Jha et al. 2020). As seen in Fig. 4, the scatter is indeed much larger than the mean. Also, a large number of BMRs are having opposite tilts (negative in the northern hemisphere) due to non-Joy and anti-Hale configurations which generate opposite polarity field. Not only the tilt, but the rate of emergence and flux content of BMR also have considerable variations around their means. The cumulative effect of the fluctuations of all these parameters of BMRs can have a large impact on the polar field or the dipole moment at the end of a cycle which can lead to a considerable variation in the solar cycle (Nagy et al. 2017). On average, in the Sun, only a few (new) BMRs per day are produced and thus the short-term variation in the poloidal field is considerably large. This we can also identify by carefully observing the magnetic field on the solar surface (Cameron et al. 2013; Jiang et al. 2014a; Mordvinov et al. 2016; Kitchatinov et al. 2018; Karak et al. 2018a; Mordvinov et al. 2022). The variation in the inflows around BMR (Jiang et al. 2010; Martin-Belda and Cameron 2017; Nagy et al. 2020) and the meridional flow (Baumann et al. 2004; Karak 2010; Upton and Hathaway 2014a) also can change the amount of poloidal field generated. Like fluctuations in the classical-α, there is a long list of work which reported the fluctuations in the Babcock–Leighton process and have utilized these in the dynamo models to reproduce various aspects of the long-term modulation of the solar cycle (e.g., Charbonneau and Dikpati 2000; Charbonneau et al. 2004; Charbonneau 2005; Charbonneau et al. 2007; Choudhuri and Karak 2009; Karak and Choudhuri 2011; Choudhuri and Karak 2012; Olemskoy and Kitchatinov 2013;

Passos et al. 2014; Lemerle and Charbonneau 2017; Karak and Miesch 2017; Nagy et al. 2017)

5.3 Time delay in various processes of the dynamo

Time delays are involved in various processes of the dynamo action. Yoshimura (1978) argued that the adjustment of the velocity field due to the back reaction of the dynamo-generated magnetic field is not instantaneous and involves a bit of delay—at low Prandtl number, the fluctuations in the large-scale flow lag behind the Lorentz force. Furthermore, the modification of the thermodynamics due to magnetic feedback alters the velocity field and this involves again a time delay. Yoshimura (1978) showed that a time delay in the dynamo model produces a long-term modulation with occasional ceased activity. In the Babcock–Leighton dynamo framework, some time delays are unavoidable because the sources for the poloidal and toroidal fields are spatially segregated. The poloidal field from the surface layer has to be transported down to the deeper CZ to be sheared by the differential rotation, thus there involves a long time lag between the poloidal to the toroidal field. This lag is comparable to the solar cycle. Similarly the toroidal to the poloidal field conversion process also involves a time lag as the toroidal field needs to rise to the surface to form BMRs and then BMRs decay to give rise to the poloidal field. This delay however is short compared to the solar cycle length as the BMR eruption takes a few days to month and the decay takes another few months. While these two lags are captured by default in the numerical dynamo models of Babcock–Leighton and interface (in cases where the regions of shear and α-effect are spatially segregated, MacGregor and Charbonneau 1997) types, a time delay is included by hand in the iterative map and the time-delay dynamo models (Sect. 5.4 of Charbonneau 2010). This time delay in the *nonlinear* dynamo model produces a variety of cycle modulations, including Gnevyshev–Ohl rule and intermittent cycles like the grand minima in certain parameter regimes (Durney 2000; Charbonneau 2001; Wilmot-Smith et al. 2006; Charbonneau et al. 2007). While in most of the Babcock–Leighton models, the toroidal to poloidal process is assumed to be instantaneous, Jouve et al. (2010) and Fournier et al. (2018) included a short delay in their model and made it magnetic field dependent regarding the fact that the flux tube with a strong magnetic field rises fast due to high magnetic buoyancy. This magnetic field-dependent time delay during the flux emergence in their flux transport dynamo with nonlinear α-effect can produce some modulation in the cycle amplitude. We here note that time delays in all these models produce cycle variability only when the nonlinearity becomes important; it is the nonlinearity which is essential to produce cycle modulation. Thus, the time delay alone cannot produce a variability in the solar cycle.

With these basic discussions of the causes of the modulation of the solar cycle, we are now ready to discuss some illustrative models for the long-term variation in the solar cycle.

6 Mean-field models for long-term cycle variabilities

6.1 Models with nonlinear feedback on the large-scale flows

As discussed in Sect. 5.1, the large-scale flows are subject to change dynamically due to direct Lorentz feedback on the flow (Malkus and Proctor 1975) or through the feedback on the angular momentum transport (like Λ effect; Kitchatinov et al. 1994b). Extensive research has been done on this topic to capture the Lorentz feedback of the dynamo-generated magnetic field (Spiegel 1977; Tavakol 1978; Ruzmaikin 1981). Particularly, using a simplified dynamo model (Küker et al. 1999) showed that a modification of the differential rotation by the large-scale Lorentz force produces strong modulation in the magnetic cycle including grand minima (also see, Moss and Brooke 2000). However, when the α quenching is added, the modulation is drastically suppressed (which is expected as the α quenching tends to limit the growth of the magnetic field). Some amount of cycle modulation and grand minima are again recovered if a strong Λ quenching is included in this model; also see Kitchatinov et al. (1999) for a similar study. In a somewhat improved dynamo model but by including only the feedback of the large-scale magnetic field on the differential rotation, Bushby (2006) find some modulation in the magnetic cycle including grand minima like phases. Chaotic solutions are also produced in the highly truncated dynamo model (Weiss et al. 1984) which produces modulation in the cycle.

Basically, in all these models, the modulations happen in two ways (Knobloch et al. 1998). In one, the large-scale magnetic field of one parity (dipolar or quadrupole) drives velocity perturbations and energy is exchanged between the magnetic field and the flow. In this case, a large variation in the flow velocity is observed with no change in the parity. In the second case, there exists a nonlinear interaction between the dipole and quadrupole modes, mediated via the velocity perturbation which is driven by the Lorentz force. This modulation is associated with changes in the parity with almost no change in the velocity (Thelen 2000). These two mechanisms of cycle modulation in the literature are referred as Type II and I, respectively (e.g., Tobias 1997; Knobloch et al. 1998). Based on a nonlinear extension of the Parker (1993) model, Beer et al. (1998) showed that the latter type of modulation is the cause of Maunder-like grand minima. In Fig. 5, we see that during the grand minimum the parity of the magnetic field is changed. Based on a highly idealized simple model of the nonlinear dynamo equations, Weiss and Tobias (2016) and Beer et al. (2018) showed that the long time-scale 'supermodulation' apparent in the cosmogenic isotope data can be ascribed to switching of the dynamo between two different modulational patterns i.e., from dipole or quadrupole symmetry to mixed-mode solutions.

Nevertheless, these models are still preliminary and fail to produce many detailed features of the observed magnetic field and the large-scale flows, particularly the correct amount of variation in the differential rotation. Furthermore, in some studies, the amount of feedback on the differential rotation and meridional circulation are tuned.

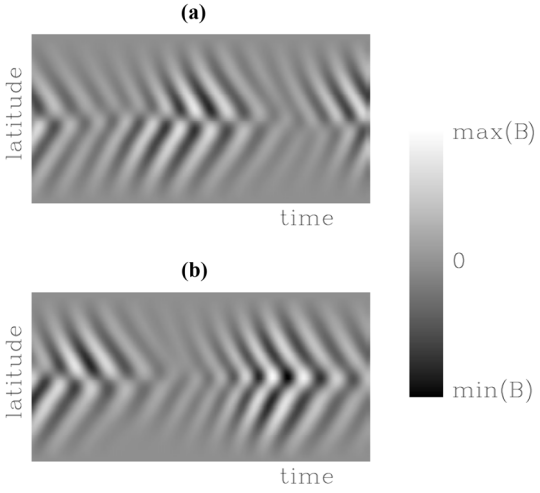

Fig. 5 Butterfly diagrams showing the toroidal field at a fixed radius as a function of time and latitude. In **a** the parity is interrupted by the occurrence of a grand minimum. The dynamo recovers from the grand minimum with a strong hemispheric asymmetry. **b** The grand minimum triggers a flip from a dipolar to quadrupolar parity. Image reproduced with permission from Beer et al. (1998), copyright by Springer

6.1.1 Variation in differential rotation

Observations find almost no variation in the differential rotation (Gilman and Howard 1984; Jha et al. 2021) except a tiny one ($<0.5\%$) around the mean, which is known as the torsional oscillation (Howe 2009). Early dynamo models tried to explain torsional oscillation using the variation of Reynolds stresses due to dynamo-generated magnetic field (Kueker et al. 1996). Some other models tried to explain it using the mean Lorentz force of the dynamo-generated magnetic field on the momentum equation (Schüssler 1981; Chakraborty et al. 2009); see Pipin and Kosovichev (2019) who included both magnetic feedbacks on the turbulent angular momentum transport and the large-scale Lorentz force. In spite of that, none of these models could successfully explain both the equatorward and poleward branches of the torsional oscillation. A comprehensive model of Rempel (2006) showed that an enhanced surface cooling of the active region belt as proposed by Spruit (2003), in addition to the Lorentz forcing, is needed to explain the equatorward branch of torsional oscillation. This model expectedly finds almost no long-term modulation in the magnetic cycle due to this tiny variation in the differential rotation. Thus, we may expect that the observed tiny change in the differential rotation may not be a potential cause of the long-term modulation in the solar cycle. However, a series of mean-field dynamo calculations have demonstrated that a variety of cycle modulations including grand minima can be produced due to the nonlinear back reaction of the magnetic field on the large-scale flow through the so-called Type I modulation, which leaves a little imprint in the differential rotation (e.g., Beer et al. 1998; Knobloch et al. 1998; Bushby 2006; Weiss and Tobias 2016). Therefore, it is subtle to answer how much is the role of the tiny variation in differential rotation in producing cycle irregularity.

6.1.2 Variation in meridional circulation

The meridional circulation is also subject to vary due to the Lorentz forcing of the dynamo-generated magnetic field acting directly on it or through the alteration of the differential rotation. Models including the magnetic feedback often find a cyclic variation in the meridional flow (Rempel 2006; Passos et al. 2012; Hazra and Choudhuri 2017), in agreement with some observations (Hathaway and Rightmire 2010). Inflows around active regions also cause a cyclic perturbation in the meridional flow (Gizon and Rempel 2008; González Hernández et al. 2008, 2010). This cyclic change in the meridional circulation with no overall modulation cannot produce much variation in the magnetic cycle (Karak and Choudhuri 2012). However, when the amount of perturbation in meridional flow varies with the solar cycle strength, it can cause a significant modulation in the solar cycle (Jiang et al. 2010). Observations find some temporal variations in the meridional circulation (González Hernández et al. 2006), although there is no consensus on its long-term trend due to limited data. If the steady-state meridional circulation is maintained by a slight imbalance between two large terms—the non-conservative part of the centrifugal force and the baroclinic forcing (which arises due to a latitudinal temperature difference), a slight change in the balance can produce a large variation in the meridional circulation (Kitchatinov and Rüdiger 1999). In fact, the global convection simulations do find a tiny variation in the differential rotation but a considerable variation in the meridional circulation (Karak et al. 2015a; Passos et al. 2017), somewhat consistent with the available observations. By assimilating the synthetic magnetic proxies in the variational data assimilation method based on flux transport dynamo model, Hung et al. (2015) and Hung et al. (2017) also find a time-varying meridional circulation.

In the models, particularly in the flux transport dynamo models, the variation in the meridional circulation has been found to produce a profound effect on the solar cycle. In these models, the meridional flow regulates the cycle duration, weaker flow makes the cycle longer and vice versa (Dikpati and Charbonneau 1999). The meridional circulation has also an effect on the cycle strength, however, the effect depends on the diffusivity used in the model. If the dynamo operates in the diffusion-dominated regime (relative importance of the diffusion is more with respect to the advection due to flow), then a weaker flow allows the poloidal magnetic field to diffuse for a longer time and thus makes the magnetic field weak (Yeates et al. 2008). The opposite scenario happens when the flow is strong. Using this idea, Karak (2010) discovered that if we want to match the cycle duration by adjusting the speed of the meridional flow, then the cycle amplitudes are also matched up to some extent. Thus, a significant part of the variation of the solar cycle can easily be modelled simply by varying the speed of the meridional flow. Karak (2010) also showed that a sudden weakening of the meridional flow can trigger a Maunder-like grand minimum as shown in Fig. 6.

Although the results from some of the flux transport dynamo models with variation in the meridional flow are very promising, in terms of modelling long-term variations in the solar cycle, it remains to be answered whether there was any large

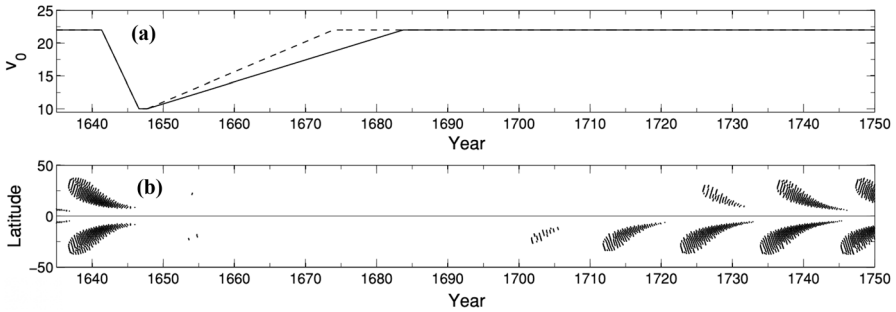

Fig. 6 Figure showing that a sufficient drop in the meridional flow can trigger a Maunder-like grand minimum. **a** Shows the required meridional circulation speed in m s^{-1} (solid/dashed for north/south). **b** Shows the location of the sunspots from the dynamo model. Image reproduced with permission from Karak (2010), copyright by AAS

variation in the meridional flow in the past, particularly during the Maunder minimum.

6.1.3 Joint models with multiple nonlinearities

A few mean-field dynamo models were developed by considering full MHD equations with multiple possible nonlinearities (Brandenburg et al. 1989, 1991; Barker and Moss 1994; Thelen 2000; Jennings 1993; Muhli et al. 1995; Rempel 2006; Pipin and Kosovichev 2019; Sraibman and Minotti 2019). Most of these models included α quenching and Lorentz force feedback (in some form) in the momentum equation. The aim of these models was mostly to study the nonlinear stability and the operation of the dynamo. These models do not produce a considerable long-term modulation and grand minima unless some stochastic fluctuations in the dynamo parameter are included (Inceoglu et al. 2017). This will be discussed in the later sections.

6.2 Models with fluctuations

As discussed in Sect. 5.2, stochastic fluctuations in the solar dynamo is unavoidable and thus using these fluctuations numerous dynamo models have been constructed to explain the variable solar cycle.

6.2.1 Fluctuations in α-effect

There is a long history studying the modulation of the solar cycle utilizing the stochastic fluctuations in the dynamo model. Choudhuri (1992), Hoyng (1993), Ossendrijver and Hoyng (1996), Ossendrijver et al. (1996), Gómez and Mininni (2006), Brandenburg and Spiegel (2008) and Moss et al. (2008) are some examples from a long list of publications in which stochastic fluctuations in the α parameter in their dynamo model were included and found long-term modulations including quiescent period like grand minima in some parameter regimes. We would like to mention that most of these models also include some nonlinearities, usually the α

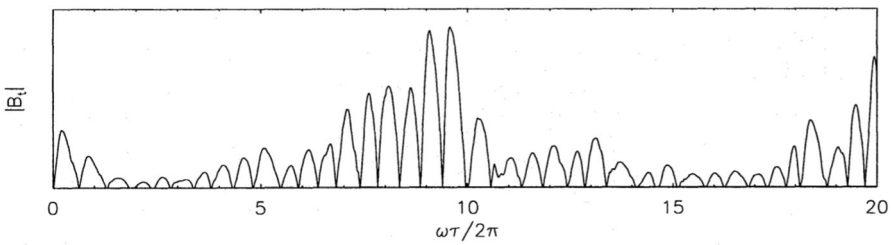

Fig. 7 A representative case of the solar cycle (as measured by the toroidal field) from a simplified αΩ dynamo model with stochastic noise in the α-effect. Image reproduced with permission from Ossendrijver and Hoyng (1996), copyright by ESO

quenching to stabilize the dynamo. Therefore, it was found that when this α quenching was included, the variability was decreased. In Fig. 7, we present cycles from a simplified mean-field αΩ dynamo model of Ossendrijver and Hoyng (1996) with stochastic fluctuations in the α term. They showed that with a certain amount of fluctuations in α, the variability in the modelled cycle closely resembles the variability seen in the observed sunspot data.

6.2.2 Fluctuations in α-effect coupled with dynamic α-effect

When the classical α-effect is combined with another α-effect having a magnetic field-dependent lower threshold, a large modulation is expected. The best example for this is the dynamo model coupled with the dynamic α-effect which is produced due to the instability in the flux tube at the BCZ (Schmitt 1985; Chatterjee et al. 2011). In a mean-field dynamo model, Schmitt et al. (1996) included this dynamic α-effect in the overshoot layer below the CZ in addition to the classical α-effect. As the dynamic α-effect works only when the magnetic field is greater than a threshold field strength, it stops operating when the field falls below this threshold. Schmitt et al. (1996) and Ossendrijver (2000) showed that when the magnetic field is strong in a normal cycle, both α operate concurrently. However, due to stochastic fluctuations, the magnetic field can occasionally fall below the threshold and the dynamical α stops operating. This caused the magnetic field to fall drastically—that is the beginning of a grand minimum; see Fig. 8. Note that in this case, the magnetic field can suddenly drop to a considerably lower value. During this quiescent period, the classical α alone slowly grows the field and recovers the model from grand minimum.

6.2.3 Fluctuations in Babcock–Leighton process

For about the last two decades, Babcock–Leighton type flux transport dynamo models have been extensively used to explain the variabilities in the solar cycle. The first landmark paper in this series came from Charbonneau and Dikpati (2000) who included stochastic fluctuations in their 2D (axisymmetric) flux transport dynamo model. For this, they added a stochastic term with a coherence time of a month in the α parameter, the Babcock–Leighton source term in their axisymmetric model. They

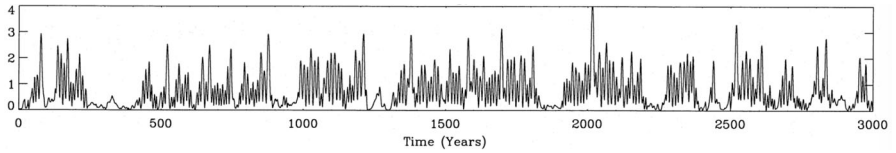

Fig. 8 Cycle modulations and grand minima (as measured by the magnetic energy) in the dynamo model with stochastic fluctuations in the α-effect combined with a (threshold field dependent) dynamic α produced due to the instability in the flux tube at the BCZ. Image reproduced with permission from Schmitt et al. (1996), copyright by ESO

essentially replaced α by $[1 + s\ \sigma(t)]\alpha$ in Eq. (11), where σ is random deviate within $[-1, 1]$ whose value is updated every month and s determines the level of fluctuations. They found some modulation in the solar cycle, including the observed weak anti-correlation between the cycle duration and the amplitude with 200% fluctuations ($s = 1$) in α. Later Charbonneau et al. (2007) showed that the long time delay inbuilt in this type of Babcock–Leighton dynamo model naturally reproduces a Gnevyshev–Ohl like pattern in the modelled solar cycle (more in Sects. 6.4 and 8.3). Fluctuations in the Babcock–Leighton process can also lead to a large variation in the poloidal field with occasional dips in the polar field (as observed in the solar magnetic field), which can lead to double peaks (Gnevyshev gaps) and spikes in the following cycle (Karak et al. 2018a). Large fluctuations in the Babcock–Leighton process also lead to Maunder-like grand minimum as shown initially by Charbonneau et al. (2004) and later by many other authors (Choudhuri and Karak 2009; Passos et al. 2012; Hazra et al. 2014b; Passos et al. 2014) in different Babcock–Leighton type dynamo models. In particular, Choudhuri and Karak (2012) estimated the amount of variation in the polar field at the end of a cycle (a cumulative effect of the fluctuations in the Babcock–Leighton process) and the variation in the meridional circulation based on indirect observations and included those into their high diffusivity dynamo model. They found the correct frequency of the grand minima in the last 11,000 years (Fig. 9). Another work was by Olemskoy and Kitchatinov (2013) who also made an estimate of the level of fluctuations in the Babcock–Leighton process by computing the contribution to the polar field from the sunspot group data of Royal Greenwich, Kodaikanal and Mount Wilson Observatories. They found that the statistic of grand minima are consistent with the Poisson random process, which indicates that the initiation of grand minima is independent of the history of the past minima (also see Karak and Choudhuri 2013). They also showed that there is a correlation between the occurrence of grand minima and the deviation from the dipolar parity and thus the hemispheric asymmetry; also see Nagy et al. (2017) and Hazra and Nandy (2019) for the same conclusion from different Babcock–Leighton models. Figure 10a shows the smoothed (in the same way as done in, Usoskin et al. 2007) sunspot number from an 11,000-year long simulation done by Olemskoy and Kitchatinov (2013) in which the red and blue shaded areas represent the grand maxima and minima, respectively.

The hemispheric asymmetry which is a robust feature during grand minima is also reflected in a typical grand minimum as presented in Fig. 10b. The fluctuations in the Babcock–Leighton process of north and south hemispheres are uncorrelated and thus

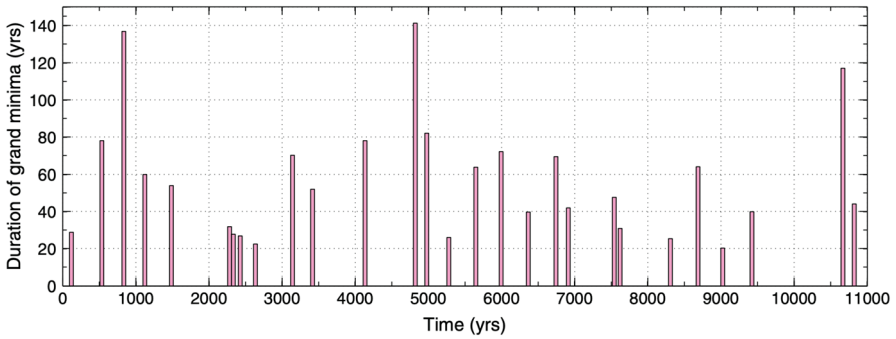

Fig. 9 The durations vs the times of their occurrence of the grand minima in the 2D Babcock–Leighton dynamo model of Choudhuri and Karak (2012). Image reproduced with permission from Choudhuri and Karak (2012), copyright by APS

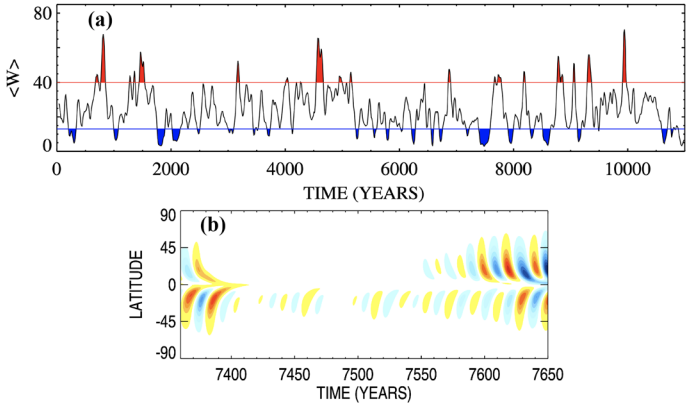

Fig. 10 **a** A proxy of the smoothed sunspot number from the dynamo model of Olemskoy and Kitchatinov (2013). Blue and red shaded regions correspond to the grand minima and maxima (using the same definition as used in, Usoskin et al. 2007). **b** Toroidal field as a function of latitude and time, highlighting a grand minimum. Images reproduced with permission from Olemskoy and Kitchatinov (2013), copyright by AAS

hemispheric asymmetry is unavoidable during grand minima in this model and also other dynamo models with fluctuations in the Babcock–Leighton process (Passos et al. 2014; Karak and Miesch 2018). The hemispheric asymmetry, however, cannot remain for multiple cycles as the diffusive coupling at the equator tends to smooth out the asymmetry acquired due to fluctuations (Chatterjee and Choudhuri 2006; Karak and Miesch 2017). Another way that north–south asymmetry in the magnetic field can come about in these models is due to the random excitation of the quadrupolar mode by the stochastic fluctuations in the Babcock–Leighton process (Schüssler and Cameron 2018).

Further support for the stochastic origin of the long-term modulation of the solar cycle came from Cameron and Schüssler (2017) who studied the following 'stochastic' normal form model.

$$dX = \left(\beta + i\omega_0 - (\gamma_r + i\gamma_i)|X|^2\right)Xdt + \sigma X dW_c = 0, \tag{13}$$

where X is a complex quantity whose real and imaginary components give the toroidal and poloidal fields, β determines the growth rate of the dynamo and thus the supercriticality, ω_0 sets the magnetic cycle frequency, γ_r and γ_i regulate the nonlinearity of the model and determine the cycle amplitude, W_c represents a complex Wiener process and σ is a measure of added noise. The values of all these parameters are fixed by the observations. Cameron and Schüssler (2017) showed that in the weakly nonlinear regime, the variability of the solar cycle as seen in the reconstructed data over the past 9000 years can be modelled using this stochastic normal-form model (Cameron and Schüssler 2019). They have also tested this idea using a 1D Babcock–Leighton type dynamo model constrained by observations.

While most of the Babcock–Leighton models are kinematic (see Bekki and Cameron 2022, for an exception to this), recently Inceoglu et al. (2017) utilized the 2D nonkinematic dynamo model of Rempel (2006) to study the nature of the grand minima and maxima. In this work, they considered random fluctuations in the angular momentum transport process in addition to the Babcock–Leighton term. This caused some nonlinear interaction between the flow and the fields. Even in this model, they found that the occurrences of grand minima and maxima are largely described by memoryless processes. In this model, it is also expected to observe modulation in the flow. They found that the radial differential rotation tends to be larger during grand maxima, while it is smaller during grand minima. The latitudinal differential rotation, on the other hand, is found to be larger during grand minima in agreement with the data by Ribes and Nesme-Ribes (1993). The meridional circulation speed tends to be faster during grand minima.

Recently, two comprehensive kinematic Babcock–Leighton dynamo models, namely, 2×2D model (Lemerle and Charbonneau 2017; Nagy et al. 2017) and 3D model (Miesch and Teweldebirhan 2016; Karak and Miesch 2017) were used to model the cycle modulations. The good thing about these models is that the BMRs are explicitly deposited in these models and thus all the observed (statistical) properties of the BMRs are captured by and large. Lemerle and Charbonneau (2017) and Karak and Miesch (2017) showed that the randomness associated with the BMR production are the major causes for the long-term modulation in the solar cycle. Both these groups included the observed scatter around Joy's law tilt (using a Gaussian distribution) and found considerable amount of variation, including north–south asymmetry and grand minima in the solar cycle (Figs. 11 and 12). As the level of fluctuations is increased, the variability and the number of grand minima is increased (Fig. 12). We note that the observed distribution in the delay time of the BMR eruption and the BMR flux also give some modulation in the solar cycle as seen in Fig. 12a in which there is no scatter imposed around Joy's law.

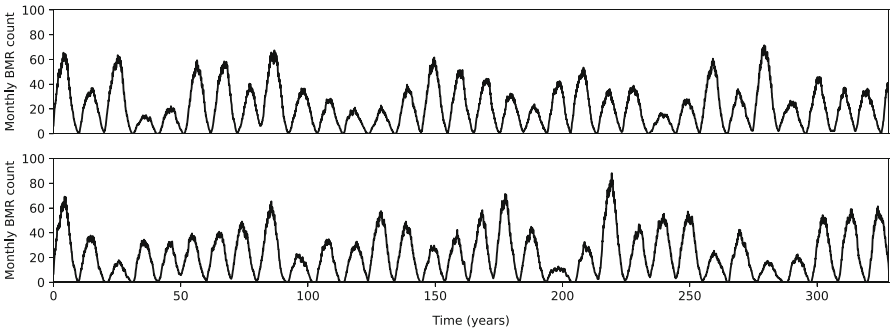

Fig. 11 Time series of the monthly BMR number (pseudo-SSN) from the simulation with observed tilt scatter of the 2 × 2D kinematic Babcock–Leighton model (Lemerle and Charbonneau 2017). Panels are obtained from two different realizations of dynamo simulations at same parameters

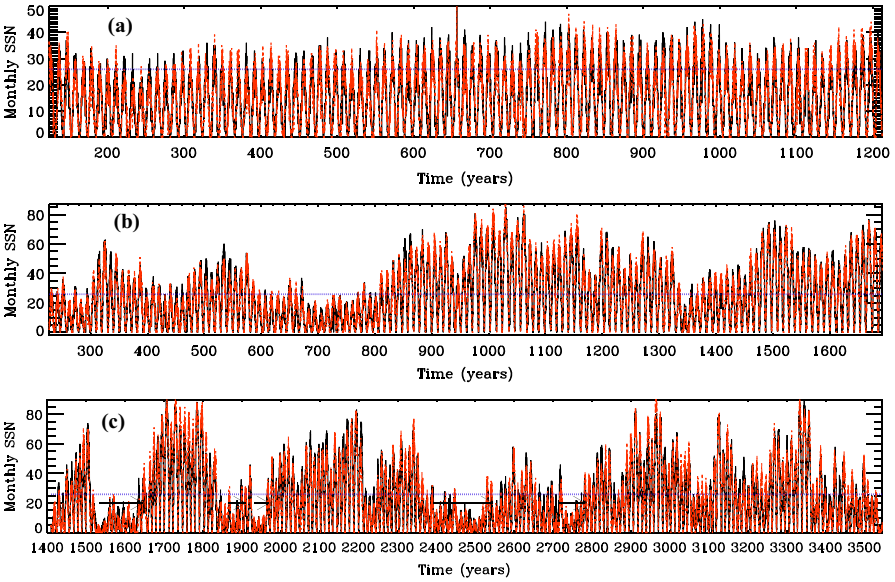

Fig. 12 Time series of the monthly BMR number from a 3D kinematic Babcock–Leighton dynamo model **a** without tilt scatter, **b** with a Gaussian scatter of $\sigma_\delta = 15°$ (close to the observed value), and (c) $\sigma_\delta = 30°$, respectively taken from Runs B9, B10, and B11 of Karak and Miesch (2017). The horizontal line shows the mean of peaks of the monthly group numbers obtained for last 13 observed solar cycles. Arrows in **c** represent the locations of grand minima. Images reproduced with permission from Karak and Miesch (2017), copyright by AAS

6.2.4 Does the Babcock–Leighton process operate during grand minima?

Dynamo models including only the Babcock–Leighton process for the poloidal source is so successful in reproducing the observed features of the solar cycle, it is

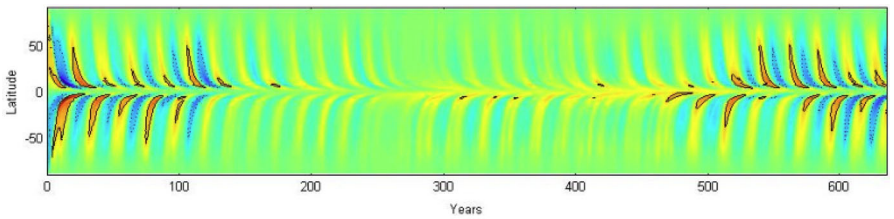

Fig. 13 Grand minima reproduced from 2D flux transport dynamo model with additional α-effect operating in the bulk of the CZ (Passos et al. 2014). Colour shows the toroidal field at the BCZ and the contours show the areas where the field exceeds the threshold for the model-spot eruptions. Note that in this model, the recovery from the grand minimum is due to the α-effect; see also Ölçek et al. (2019). Image reproduced with permission from Passos et al. (2014), copyright by ESO

natural to ask the question whether the Babcock–Leighton process operates during grand minima.

To operate the Babcock–Leighton process, we need "tilted" BMR. However, observations, particularly the early ones, found only a few spots during the Maunder minimum. Thus, one would expect that the Babcock–Leighton process will not operate, or be inefficient during the Maunder minimum and possibly during other grand minima. The classical (helical) α (Parker 1955a) which efficiently operates in the sub-equipartition field is a obvious candidate for the generation of the poloidal field during these episodes (Karak and Choudhuri 2013; Hazra et al. 2014b). Passos et al. (2014) performed simulations of 2D Babcock–Leighton dynamo model with a weak classical α operating in the whole CZ. They showed that this additional α produces poloidal field and recovers the model from grand minima when the Babcock–Leighton process stops operating (Fig. 13); also see Ölçek et al. 2019 for another beautiful demonstration of this idea in 2D×2D model with explicit BMR deposition. Unlike most of the Babcock–Leighton dynamo models,[2] in these models, the Babcock–Leighton process is stopped operating at low field regime by introducing a lower threshold and thus only helical α operates during grand minima. The mechanism of this type of dual dynamo model is similar to the model of Ossendrijver and Hoyng (1996) in which a classical α and the dynamical α driven by the magnetic buoyancy were incorporated (Sect. 6.2.2).

In any rotating convective layer (like the solar CZ), generation of α-effect is natural. However, its nature and how strong its value in the CZ is still uncertain. Thus introducing this α in the model, brings several unknown parameters. On the other hand, the following facts support the operation of Babcock–Leighton process during Maunder minimum and other grand minima. (1) Maunder minimum was not completely devoid of sunspots. Recent analyses clearly show that some spots were observed during the Maunder minimum (Zolotova and Ponyavin 2015; Usoskin et al. 2015; Vaquero et al. 2015; Zolotova and Ponyavin 2016). (2) Even a few BMRs can produce an appreciable amount of poloidal field which, if not decayed considerably,

[2] Even the models of grand minima by Karak (2010), Choudhuri and Karak (2012) and Karak and Choudhuri (2013) using the Surya code (Chatterjee et al. 2004) although include a lower threshold for the spot eruption, the Babcock–Leighton process still operates in these models because some toroidal field rises to the upper layer due to upward meridional flow and diffusion.

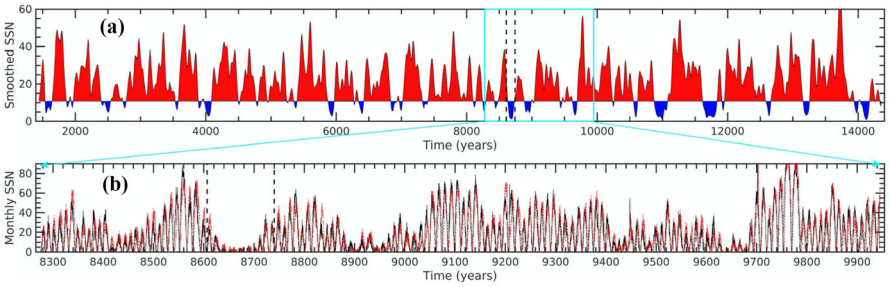

Fig. 14 **a** Decadal-binned and smoothed BMR number from the model of Karak and Miesch (2018) with randomness in the BMR properties (mainly scatter around Joy's law tilt). **b** Shows the zoomed-in portion of the monthly smoothed BMR number. Image reproduced with permission from Karak and Miesch (2018), copyright by AAS

can slowly produce enough toroidal field and recover the Sun from grand minima phase. In fact, Cameron et al. (2012) showed that in the Sun the diffusion of the poloidal field through the surface is negligible—this in the flux transport dynamo models can be achieved by including a downward magnetic pumping (Karak and Cameron 2016). (3) Smaller BMRs (including ephemeral regions) produce little contrast in the white light and were not detectable as spots with the telescopes of the Maunder minimum epoch (Jha et al. 2020) but their eruption rate is large (smaller the BMR, larger is the emergence rate; Hagenaar et al. 2003). These small BMRs have some non-zero tilt and they can produce some polar field during grand minima (Stenflo and Kosovichev 2012; Tlatov et al. 2013; Jha et al. 2020).

By including a downward magnetic pumping, Karak and Miesch (2018) showed that the model with stochastic properties (tilt scatter) in BMRs can recover from grand minima without any additional source for the generation of the poloidal field; see Fig. 14. They found that during grand minima as the poloidal magnetic field does not decay (due to pumping), it keeps on supplying the toroidal field and thus the model continues to produce BMR at a low rate even during grand minima (Fig. 15). The poloidal field generated from these few BMRs is alone sufficient to recover the model to the normal phase. Their model reproduces most of the features of the grand minima (including frequency of grand minima, longer cycles and strong hemispheric asymmetry during grand minima).

6.2.5 Variability vs dynamo supercriticality

Whenever there is any change in the dynamo number D ($= \alpha_0 \Delta\Omega R_\odot^3/\eta_0^2$, where α_0 is the strength of α-effect, $\Delta\Omega$ is the amount of shear in the CZ, and η_0 is the diffusivity), there will be a change in the amplitude of the magnetic field. Thus, the cycle modulation due to fluctuations in the dynamo parameter is obvious. However, for a given level of fluctuations and the form of nonlinearity, the amount of variability depends on the value of D or the regime operation of the dynamo. This is apparently seen in Fig. 16 that the same amount of variation in D causes a large variation in magnetic field when the dynamo operates near the critical transition

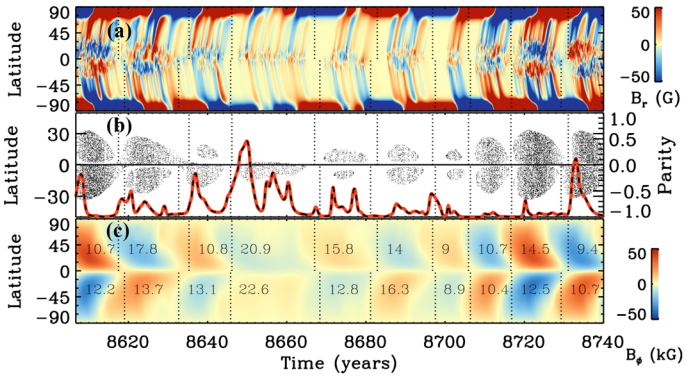

Fig. 15 Evolution of the **a** surface radial field **b** BMR eruptions and the hemispheric parity of the toroidal field (dashed line) and **c** the toroidal field at BCZ from a grand minimum presented in Fig. 14b (marked by dashed lines). Image reproduced with permission from Karak and Miesch (2018), copyright by AAS

($\delta|B_c|$) and a small variation when the dynamo operates in supercritical regime ($\delta|B_s|$).[3] The reason for this is not difficult to understand. When the dynamo operates near the critical transition, a small D makes the growth rate of the magnetic field small and the dynamo weakly nonlinear. Now consider a scenario when the magnetic field has become weak due to a reduction of D (or α_0) and after some time due to fluctuations, D has increased. Then the dynamo will (almost linearly) amplify the field for a long time before the nonlinearity becomes important and thus the net growth of the field will be large. On the other hand, if the dynamo operates in a highly supercritical regime, then the nonlinearity will quickly suppress the dynamo growth and the net amplification of the field will be small.

The above discussion also means that in the near-critical (or weakly supercritical) regime, we expect long-term modulation in the cycle and extended grand minima. In this regime when the field becomes weak due to fluctuations, the dynamo will take a long time (several cycles) to grow the field and this will tend to produce a smooth long-term variation. In contrast, in the super-critical regime, we do not expect much long-term modulation in the cycle amplitude and no extended grand minima because when the magnetic field falls to a low value, the dynamo will quickly increase the field in a cycle. This is clearly seen in Fig. 17; also see Vashishth et al. (2021), Tripathi et al. (2021) and Albert et al. (2021). Furthermore, for the given diffusive and advective transports, the long-term memory of the field should depend on the supercriticality of the dynamo. Kumar et al. (2021a) showed that in the weakly supercritical dynamo, the long-term memory of the polar field persists for multiple cycles. However, when the supercriticality is increased, the multi-cycle memory is reduced to only one cycle. In fact, for rapidly rotating young stars, we expect the dynamo to be strong (convective motion is more helical) and thus we do not expect extended grand minima there (Vashishth 2022; Vashishth et al. 2023). This is

[3] Another way to understand this result is from the dynamo instability. In a slightly supercritical regime, the amplitude B of magnetic cycles follows a general rule $B \propto (D - D_c)^{1/2}$ for all instabilities (Landau and Lifshitz 1987). Thus, $\delta B/\delta D$ decreases with the supercriticality.

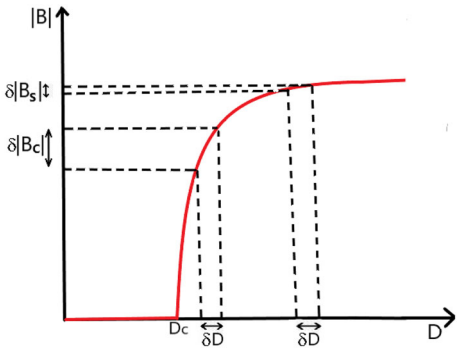

Fig. 16 A Hopf bifurcation diagram, showing the transition from a fixed point to dynamo instability. This is a typical variation of the magnetic field strength ($|B|$) vs dynamo number (D) in dynamo model with any nonlinear quenching mechanism as long as D is not much larger than D_c. Here, D_c is the critical D. $\delta|B_c|$ and $\delta|B_s|$ are the amplitude variations of the magnetic field for a given change in D in two different regimes of the dynamo

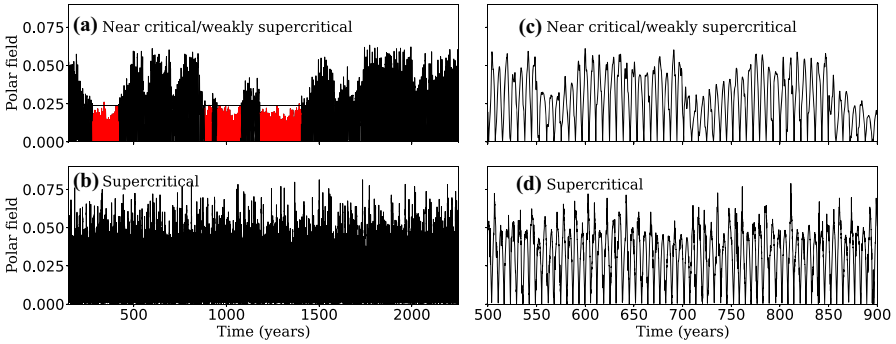

Fig. 17 Polar field (averaged over 55° latitude to north pole) from a dynamo simulation in which the dynamo operates **a** near-critical or weakly-supercritical regime ($D/D_c = 2$) and **b** supercritical regime ($D/D_c = 6$). **c** and **d** are showing the cycles for 400 years from the long data shown in (**a**) and (**b**), respectively. The red portions represent extended weaker activity (the grand minima). The figures are produced from the model presented in Kumar et al. (2021a)

congruous with the stellar observations that the grand minima are detected only in the slowly rotating stars (Boro Saikia et al. 2018; Oláh et al. 2016; Shah et al. 2018; Garg et al. 2019; Baum et al. 2022).

The above discussion, although seems to be promising, has a subtlety. In the highly supercritical regime, when the dynamo number is increased to a very high value, the variability of the magnetic field may not remain small because the dynamo may enter into a more complex regime. In this regime, dynamo modes with different base periods can emerge and in turn the linear superposition and nonlinear coupling of different modes is expected to introduce an increasingly strong and complex modulation of the periodic behaviour (Charbonneau et al. 2007; Schüssler and Cameron 2018; Albert et al. 2021). In addition, even without the presence of other

modes and other base periodicities, the iterative map of Charbonneau (2001) and the flux transport dynamo model inbuilt with a time delay and nonlinearity (Charbonneau et al. 2005) enter into chaotic solution through sequence of period-doubling bifurcations. However, we must remember that to enter the dynamo into this region, the D must be much larger than D_c; see e.g., Fig. 3 of Charbonneau et al. (2005); also see the discussion given at the end of Sect. 5.1. Furthermore, we find that Babcock–Leighton dynamos with the popular α-quenching of the form: $1/[1 + (B/B_0)^2]$ does not lead to chaotic solution; the solution remains stable all the way to a very large value of D.

It remains a big question that what is the supercriticality of the Sun. Stellar observations indicate that probably our Sun is not too supercritical (Metcalfe et al. 2016; Kitchatinov and Nepomnyashchikh 2017). Furthermore, as only the weakly supercritical dynamo produces grand minima (Vashishth et al. 2021; Kumar et al. 2021a; Cameron and Schüssler 2017) and somewhat smooth cycle variation and Sun does produce grand minima, we expect that the solar dynamo is probably not operating in highly supercritical regime.

6.3 Specific nonlinearities in the Babcock–Leighton process

In the Babcock–Leighton solar dynamo also, the magnetic field acts on the flow and gives a nonlinearity in the model. However, given the fact that the observed differential rotation has only a little variation over the solar cycle, the poloidal to toroidal field conversion, i.e., the Ω effect, is largely linear. On the other hand, the toroidal to poloidal part of the Babcock–Leighton models is not due to the classical α-effect which experiences a catastrophic quenching due to magnetic helicity conservation (Sect. 8.7 of Brandenburg and Subramanian 2005), rather it is due to the Babcock–Leighton process. The latter is a nonlocal process and does not experience catastrophic quenching (Kitchatinov and Olemskoy 2011a). However, due to a lack of understanding in the past, most of the Babcock–Leighton dynamo models included a simple quenching of the form $1/\left(1 + (B/B_0)^2\right)$ in the poloidal field term to limit the growth of magnetic field (Charbonneau 2020). Fortunately, in recent years some potential candidates for nonlinearity have been identified which we discuss below.

6.3.1 Tilt quenching

The tilt angle of BMR plays a crucial role in generating the poloidal field in the Sun. Theory based on the thin flux tube approximation suggests that the tilt is produced due to the torque induced by the Coriolis force acting on the east–west flow emerging from the apex of the rising flux tube of toroidal field (D'Silva and Choudhuri 1993; Fan et al. 1994, also see Sect. 5 of Fan 2021). If a flux tube has a strong magnetic field, then there will be two consequences. One is that the flux tube will rise quickly due to strong magnetic buoyancy and thus the Coriolis force will not get much time to induce the tilt. The other consequence is that the flux tube will have strong magnetic tension which will oppose the torque. Both of these effects will reduce the

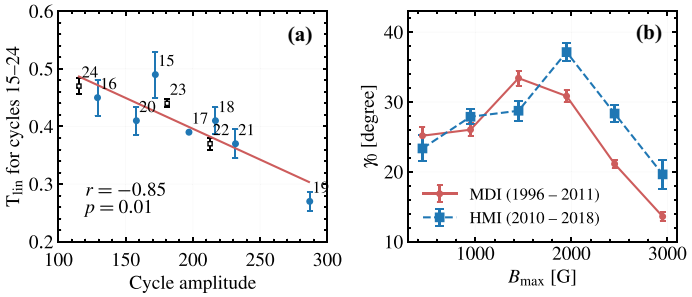

Fig. 18 **a** Tilt coefficient as computed from the mean tilt normalized by the mean latitude vs the sunspot cycle amplitude (Jiao et al. 2021); also see Dasi-Espuig et al. (2010). **b** Slope of Joy's law as a function of the maximum field strength of the BMR (Jha et al. 2020)

tilt. Based on this theoretical concept, we expect the tilt to decrease with the magnetic field in the BMR forming flux tube. This, the so-called tilt quenching may be a potential source for the nonlinearity in the Babcock–Leighton type dynamo models.

The observational support for the tilt quenching however is limited. Dasi-Espuig et al. (2010) have found an anti-correlation between the cycle amplitude and the cycle-average tilt angle of the sunspot group normalized by the mean latitude from the white-light data of Mount Wilson and Kodaikanal Solar Observatories (also see Dasi-Espuig et al. 2013 for the corrected plot for Mount Wilson data). However, other studies do not find a statistically significant relationship for this (e.g., Wang et al. 2015). Also, studies have shown that the tilt angle measured from the white light data can be significantly different than that obtained from the magnetic field data (Poisson et al. 2020). Jiao et al. (2021) carefully examined the previous methods of estimating tilt angles from Kodaikanal and Mount Wilson, supplemented by tilt angles from Debrecen Photoheliographic data and show that the tilt is statistically anti-correlated with the cycle strength as shown in Fig. 18a.

While the above studies explored the variation of the cycle-average tilt with the cycle strength, Jha et al. (2020) examined the tilt of BMR within the cycle from the line-of-sight magnetograms of Michelson Doppler Imager [MDI onboard Heliospheric Observatory (SOHO); 2010–2018] and Helioseismic and Magnetic Imager [HMI onboard Solar Dynamic Observatory (SDO); during 1996–2011]. They showed that the BMR tilt has non-monotonous dependence on the BMR's field strength; in the small field regime, the tilt increases and in the large field regime it decreases. This is shown in Fig. 18b. We note that in this study, the data were used from Cycles 23 and 24 which are weak cycles and for these very little reduction of tilt was seen in the study of Jiao et al. (2021). Therefore, the limited data used in Jha et al. (2020) could not predict the exact magnetic field-dependent form of the BMR tilt.

6.3.2 Flux loss due to magnetic buoyancy

Magnetic buoyancy is the key for the formation of sunspots or more generally BMRs (Parker 1955b). Models under thin flux tube approximation showed that when a

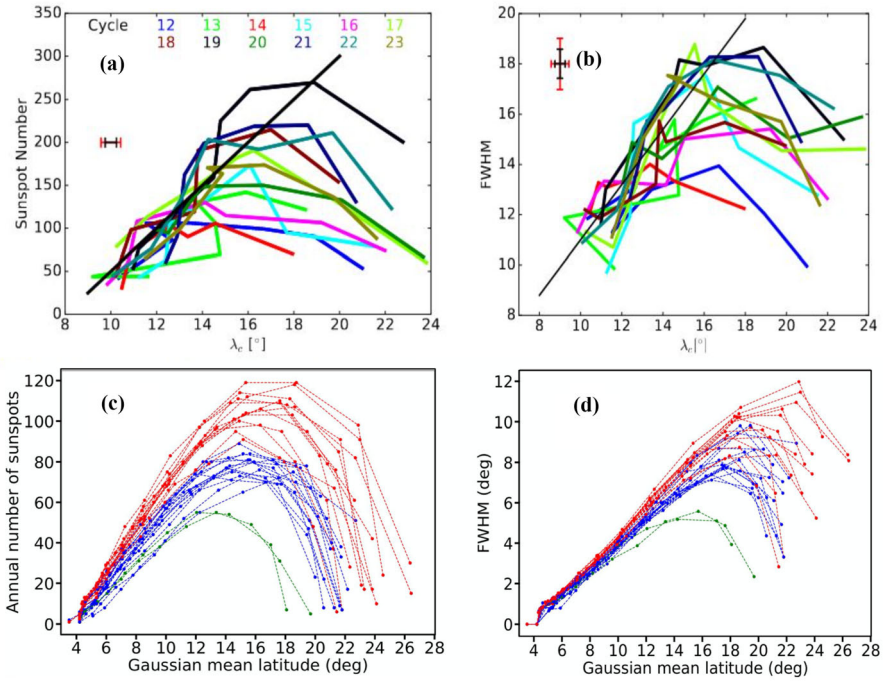

Fig. 19 The trajectory of the cycles when plotted in terms of annual sunspot number (**a**, **c**) and full width at half maximum (FWHM) of the latitudinal distribution (**b**, **d**) against the central latitude of the annual distribution. **a**, **b** From observations. **c**, **d** From dynamo simulation with buoyancy-induced toroidal flux loss. The plots show that the beginning phases (right part of the curves) of the cycles are widely different depending on their strength yet the decline phase are quite similar irrespective of their strength. Also see Talafha et al. (2022) for modeling these features using a different model. Images reproduced with permission from [top] Cameron and Schüssler (2016), copyright by ESO; [bottom] Biswas et al. (2022), copyright by APS

portion of the toroidal flux tube with sufficient field strength at the BCZ becomes magnetically buoyant, it rises to surface to give rise to a BMR. In this process, the portion of the flux tube from where the flux is depleted becomes inefficient for flux eruption for some time. As the flux emergence happens only when the field strength exceeds a certain value and after each flux emergence the flux is reduced locally, this introduces a nonlinearity in the dynamo. This nonlinear loss of toroidal flux plays an important role in limiting the growth of the magnetic field in the Sun (Schmitt and Schüssler 1989; Nandy and Choudhuri 2000; Chatterjee et al. 2004). Studies have shown that dynamo models including magnetic buoyancy reproduces observations better (Schmitt and Schüssler 1989; Hazra et al. 2015).

By introducing the magnetic buoyancy in a simple way, Biswas et al. (2022) explained the observed latitudinal variation of the solar activity over the cycle as shown in Waldmeier (1955) and Cameron and Schüssler (2016) also see Fig. 19a, b. Let us explain how the flux loss helped to explain the observed feature. In the Babcock–Leighton dynamo model, the poloidal magnetic field largely produces a toroidal field in the higher latitudes of the deeper CZ and then this toroidal field is

advected towards the lower latitudes. During its journey, when the toroidal field exceeds a certain value B_c (the threshold for BMR eruption), it starts producing BMRs at higher latitudes. As the Ω effect keeps on producing the toroidal field, the activity grows while the toroidal flux is advected towards the equator. Now consider a cycle becomes strong. The strong cycle starts producing BMRs at high latitudes and the activity (number of BMR) rises rapidly (strong cycles rise rapidly). Rapid growth means the toroidal flux loss occurs at a faster rate. Quickly the magnetic field at BCZ becomes comparable to B_c and the activity does not grow further. Any further generation of the magnetic field will then be compensated by the flux loss due to BMR emergence and the cycle decline at the same rate for all cycles; Fig. 19c, d. That is why in strong cycles the activity begins to decline when the activity belt is already at higher latitudes.

We would also like to mention that without invoking the flux loss due to magnetic buoyancy, only the cross-equatorial diffusion was used to explain this universal decline of the solar activity in different studies (Cameron and Schüssler 2016; Talafha et al. 2022).

6.3.3 Latitudinal quenching

The observational facts presented in Fig. 19a, b also suggest that strong cycles on average produce BMRs at high latitudes and vice versa (also see Waldmeier 1955; Solanki et al. 2008; Mandal et al. 2017). On the other hand, we know that when BMRs appear at higher latitudes, they are less efficient in generating a poloidal field due to poor cross-equatorial cancellation (Jiang et al. 2014a; Karak and Miesch 2018; Petrovay et al. 2020). In contrast, when BMRs appear near the equator, it becomes easier for the leading polarities to cancel with the flux of the opposite polarity from the other hemisphere. Now consider a cycle that has become strong in which the BMRs appear in high latitudes. These high latitudes BMRs will produce less poloidal field and the next cycle will be weak. Hence, the indefinite growth of the magnetic field will be halted. Petrovay (2020) called this mechanism latitude quenching and Jiang (2020) argued that this mechanism could stabilize the growth of the magnetic field in the kinematic dynamo. Karak (2020) implemented this idea in a 3D Babcock–Leighton dynamo model by taking a simple latitude-dependent threshold for BMR eruption and showed that this latitudinal quenching can regulate the growth of the magnetic field when the dynamo is not too supercritical.

6.3.4 Magnetic field-dependent inflows around BMRs

Surface observations show a converging flows around the BMRs (Gizon et al. 2001; González Hernández et al. 2008). These inflows cumulatively generates mean flows around the activity belt whose strength depends on the amount of flux in the cycle (Jiang et al. 2010; Cameron and Schüssler 2012). Due to these flows, the cross-equatorial cancellations of the BMRs are reduced and the effectivity of the Babcock–Leighton process is suppressed. In a strong cycle, this effect is stronger and thus lead to a stabilizing effect in the dynamo (Martin-Belda and Cameron 2017; Nagy et al. 2020).

In summary, tilt quenching, flux loss due to magnetic buoyancy, latitudinal quenching and inflows are the potential candidates for the nonlinearity in the toroidal to the poloidal process of the Babcock–Leighton dynamo which can potentially saturate the magnetic field.

6.4 Time-delay models

As discussed in Sect. 5.3, the time delay involved in various processes in the solar dynamo, operating concurrently with the nonlinearity can lead to irregular cycles. Yoshimura (1978) introduced a long delay of 29 years in the nonlinear dynamo model and found occasional eras of suppressed activity. Although such a long delay is not expected in the solar dynamo, a finite delay arises naturally in any dynamo model as long as the sources for the poloidal and toroidal fields are spatially segregated. In the Babcock–Leighton dynamo models, the poloidal field after it is produced near the surface through the decay of tilted BMRs needs to be transported to the deeper CZ (through meridional circulation, turbulent diffusion and pumping) where the toroidal field is generated through the Ω effect. There is also a short time delay between the toroidal and poloidal field conversion as the toroidal flux tubes take finite time to rise to the surface to form BMR and a finite time is spend to decay and disperse the BMR. All these two delays in the nonlinear dynamo model can produce a variety of modulations.

6.4.1 Iterative map

Durney (2000) assumed that there is a delay of one cycle between the poloidal field of cycle n and the toroidal field of cycle $n+1$ and brilliantly reduced the Babcock–Leighton dynamo equations into a iterative map. He writes,

$$T_{n+1} = \Delta\Omega \Delta t P_n = a P_n, \qquad n = 0, 1, 2, \ldots \tag{14}$$

(Here $\Delta\Omega$ is the shear in the CZ and Δt is the time interval during which the poloidal field acts on the shear.) Neglecting the time delay in the toroidal to poloidal fields conversion, we can write the following nonlinear relation:

$$P_{n+1} = f(T_{n+1}) T_{n+1} \tag{15}$$

Here $f(T_{n+1})$ is a measure of the efficiency of the poloidal field generation from the toroidal field (Babcock–Leighton process) which depends on the toroidal field. Substituting Eqs. (14) into (15) and normalizing the fields appropriately, we find

$$p_{n+1} = a f(p_n) p_n \tag{16}$$

(where normalizing factors are absorbed in a). For different nonlinear functions (f) of the Babcock–Leighton process, different maps can be constructed. Durney (2000) chose it $1 + \beta(1 - p_n)$ and thus the map became

$$p_{n+1} = p_n(1 + \beta(1 - p_n)) \qquad \beta > 0. \tag{17}$$

Charbonneau (2001) chose it $\gamma(1 - p_n)p_n$ which produced a map

$$p_{n+1} = \gamma\, p_n^2(1 - p_n) \qquad \gamma > 0. \tag{18}$$

By capturing a lower cut off in the Babcock–Leighton process, Charbonneau et al. (2005) produced another map

$$p_{n+1} = \alpha f(p_n)p_n \qquad \alpha > 0, \tag{19}$$

where

$$f(p_n) = \frac{1}{4}\left[1 + erf\left(\frac{p_n - p_1}{w_1}\right)\right]\left[1 - erf\left(\frac{p_n - p_2}{w_2}\right)\right] \tag{20}$$

(Here $p_1 = 0.6$, $w_1 = 0.2$ $p_2 = 1.0$, and $w_1 = 0.8$.)

Charbonneau (2001) and Charbonneau et al. (2005) showed that as the map parameter increases, the transition from the fixed amplitude oscillation to the chaotic solution occurs through a sequence of period doubling; see left panel of Fig. 20 for the map given by Eq. (19). Durney (2000) showed that in the parameter regime of the doubly periodic oscillations, the Gnevyshev–Ohl rule can be explained. Later Charbonneau (2001) showed that this is indeed not necessary, stochastic perturbation outside this region can also produce Gnevyshev–Ohl rule as a consequence of the oscillatory nature of the convergence to the fixed point; even the map without showing limit cycle for $1/(1 + B^2)$ type nonlinearity also show Gnevyshev–Ohl rule. Intermittent and chaotic solutions are produced in all these maps, as long as the map parameter is above a certain value; also see Fig. 5 of Charbonneau (2001) for an illustration.

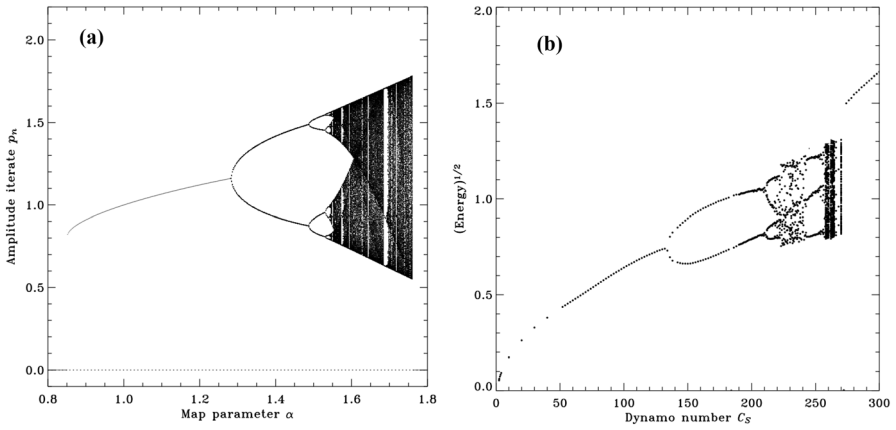

Fig. 20 Bifurcation diagrams. **a** Cycle amplitude (iterate P_n) versus the map parameter α from Eq. (19). **b** Same as left one but obtained from 2D numerical dynamo model of Charbonneau et al. (2005) and shows the magnetic energy as function of the dynamo number C_s. Images reproduced with permission from Charbonneau et al. (2005), copyright by AAS

6.4.2 1D time-delay dynamo

Finite delays are also included in the 1D dynamo models in which the equations for the toroidal and poloidal fields are truncated by removing the spatial dependences in the following way.

$$\frac{\mathrm{dB}}{\mathrm{dt}} = \frac{\omega}{L} A(t - T_0) - \frac{B}{\tau_d} \tag{21}$$

$$\frac{\mathrm{dA}}{\mathrm{dt}} = \alpha_0 f(B(t - T_1)) B(t - T_1) - \frac{A}{\tau_d}. \tag{22}$$

Here, T_0 and T_1 represent the time delays required for the generation of toroidal and poloidal fields, respectively. ω and L are the contrast in differential rotation and the length scale in the tachocline, τ_d is the diffusion time scale, α_0 is the amplitude of the Babcock–Leighton source. $f(B(t - T_1))$ is the nonlinear function which represents the suppression of the Babcock–Leighton mechanism. By considering $f(B(t - T_1))$ of the from of Eq. (20) (with lower quenching), Wilmot-Smith et al. (2006) found irregular cycles in a certain parameter regime (when the time delay is larger than the diffusion time). Later, including fluctuations in the α_0 term, Hazra et al. (2014b), Kumar et al. (2021a) and Tripathi et al. (2021) obtained long-term modulations and grand minima like intermittent solutions in a range of parameters.

6.4.3 2D time-delay dynamo

In models like the Babcock–Leighton type flux transport and the interface dynamos, in which the source regions for the fields are spatially segregated, the time delays are by default inbuilt into the equations. Thus all the Babcock–Leighton dynamo models discussed in this review are also time-delay models. Charbonneau et al. (2005) showed that the 2D Babcock–Leighton dynamo models also show the same type of behaviour as seen in the reduced map. Figure 20b, shows the bifurcation diagram of a 2D Babcock–Leighton dynamo model with a nonlinear quenching function of the form given by Eq. (20). Again, with this type of nonlinearity, we observe that the solution goes to a chaotic regime through a sequence of period doubling with the increase of dynamo number. The model is capable to produce Gnevyshev–Ohl rule in a wide range of parameter regimes with stochastically forced α (Charbonneau et al. 2007); more in Sect. 8.3.

Jouve et al. (2010) went one step ahead of this and included the short time delay associated with the flux emergence from the deep-seated toroidal flux that is usually ignored in the dynamo models. They realized the fact that the buoyancy time delay depends on the magnetic field strength—strong flux tubes experience strong buoyancy and thus rise quickly compared to the weaker ones (Fan et al. 1994). Jouve et al. (2010) captured this delay in their flux transport dynamo model by replacing the poloidal source term: αB in Eq. (11) by

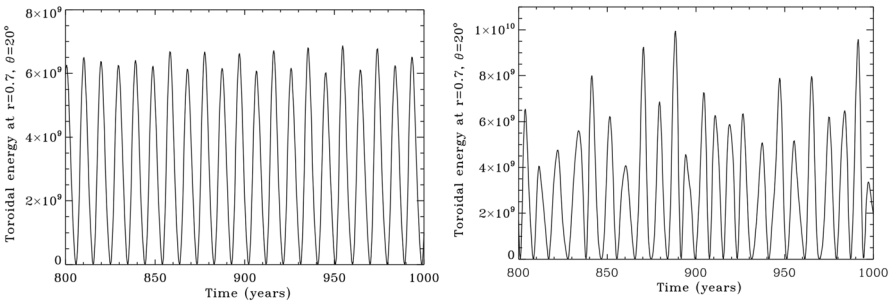

Fig. 21 Cycle modulations (as measured by the toroidal field at $r = 0.7\,R_\odot$ and $\theta = 20°$) in the flux transport dynamo model of Jouve et al. (2010) with magnetic field-dependent delay in the Babcock–Leighton source for the poloidal field generation process (Eq. 23). The left and right panels are for short (14 days on 1 kG fields) and long delay (14 days on 50 kG fields so that 10 kG fields will be delayed by almost a year in this case compared to a few hours in the previous case). Images reproduced with permission from Jouve et al. (2010), copyright by ESO

$$\frac{\alpha B(0.7\,R_\odot, \theta, t-\tau_{\rm B})}{1+(B(0.7\,R_\odot, \theta, t-\tau_{\rm B})/B_0)^2}, \tag{23}$$

where $\tau_{\rm B}$ is the delay time which they took to be equal to $\tau_0/B(0.7\,R_\odot, \theta, t)^2$ and τ_0 is used to regulate the amount of delay. Figure 21 shows the results from two simulations with different amounts of delay as presented by Jouve et al. (2010). We evidently see that just the addition of this delay in the poloidal source produces a considerable amount of modulation in the cycle and the amount of modulation increases with the increase of delay (also see Fournier et al. 2018).

However, we note that in these models, the flux loss due to magnetic buoyancy is ignored (Sect. 6.3). The flux loss tries to keep the magnetic field around the equipartition value. In that case, the toroidal flux tube will not have much different field strength from one another and the delay times will not be very different. Hence, if the flux loss due to magnetic buoyancy is incorporated in these models then we do not expect much modulation in the cycle. Biswas et al. (2022) included flux loss due to magnetic buoyancy in the dynamo model with local α prescription and they did not find noticeable modulation in the cycle due to field-dependent delay with respect to the case without delay.

7 MHD simulations for long-term cycle variabilities

In the MHD simulations one needs to solve the following continuity equation for the mass and the energy equation in addition to Eqs. (1) and (2).

$$\frac{\partial \rho}{\partial t} + \boldsymbol{\nabla}\cdot(\rho \boldsymbol{v}) = 0, \tag{24}$$

$$T\left[\frac{\partial s}{\partial t}+(\boldsymbol{v}\cdot\boldsymbol{\nabla})s\right]=\frac{1}{\rho}\left[\eta\mu_0\boldsymbol{J}^2-\boldsymbol{\nabla}\cdot(F_{\rm rad}+F_{\rm SGS})-F_{\rm cool}\right]+2\nu\boldsymbol{S}^2, \tag{25}$$

where ρ is the density, ν is the kinematic viscosity, $F_{\rm rad}$ is the radiative diffusive flux and is given by $-K\boldsymbol{\nabla}T$, K being the heat conductivity, $F_{\rm SGS}$ represents the additional subgrid scale (SGS) diffusion which is used to keep the simulation numerically stable (usually taken as $-\chi_{\rm SGS}\rho T\boldsymbol{\nabla}s'$ with $\chi_{\rm SGS}$ being the SGS diffusion coefficient and s' is the fluctuations of entropy), and $F_{\rm cool}$ is the radiative cooling near the surface. These equations are numerically solved using appropriate initial and boundary conditions to study the dynamo problem; see for example Käpylä et al. (2020) for the detailed profiles of all the model parameters and the boundary conditions.

In the last one decade, global MHD convection simulations have reached to a somewhat realistic level (not in terms of the Reynolds numbers but in terms of the level of turbulence and the realistic value of Rossby number). They produced some basic features of the large-scale flows and the magnetic field. We refer the readers to Sect. 6 of Charbonneau (2020) for a review on this subject. An advantage of these simulations is that all the nonlinear and stochastic effects are included by default in these simulations, in contrast to the mean-field models where these effects need to be included by hand. However, due to limited computation facilities, global convection simulations were rarely run for a longer time so that a long-term cycle modulations can be studied. Furthermore, being extremely complicated in nature, identifying the mechanisms of the long-term modulations are not trivial. Fan and Fang (2014), Karak et al. (2015a), Viviani et al. (2018) and Viviani et al. (2019) presented some simulations which were run for a somewhat longer duration. Here we discuss three important results for the cycle modulations gleaned from three different numerical codes. The first one is from Passos and Charbonneau (2014) who presented cycles from a simulation run of 1650 years in which 40 excellent cycles with average period of 40 years were seen (Fig. 22). This simulation 'broadly' reproduces some observed features of the solar magnetic cycle including the regular polarity reversal and dipole-dominated large-scale field. Interestingly a good amount of modulation in the cycle amplitude is naturally produced in this simulations. There is also a pattern for the Gnevyshev–Ohl rule (watch the peaks after $t = 800$ yr) and a hint for the Gleissberg modulation in these cycles. However, in this 1650 years of simulations no grand minimum or maximum is seen. With respect to the solar observations, there are some discrepancies as well which include an in-phase variation of the poloidal and toroidal

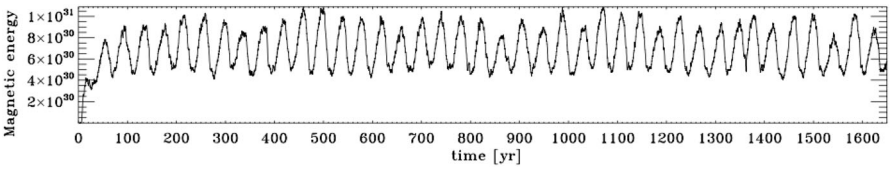

Fig. 22 Cycles from the global MHD convection simulations using EULAG-MHD code. Image reproduced with permission from Passos and Charbonneau (2014), copyright by ESO

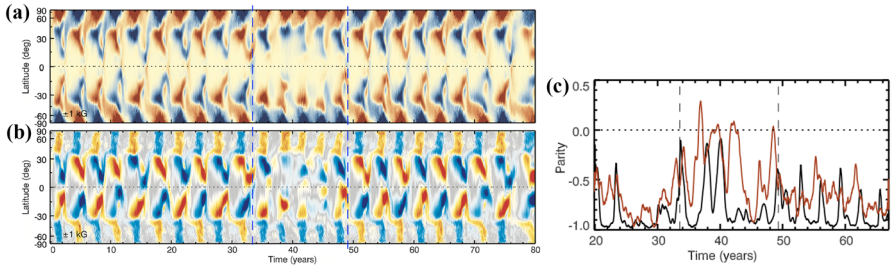

Fig. 23 Left top: Time-latitude distributions of the longitude average B_r and B_ϕ at $0.92\,R_\odot$ from the ASH simulation code of Augustson et al. (2015). The grand minimum identified in this simulation is marked by vertical lines. Right panel shows the parity of the magnetic field computed at $0.75\,R_\odot$ (orange curve) and $0.95\,R_\odot$ (black). Images reproduced with permission from Augustson et al. (2015), copyright by AAS

components, magnetic activity confined to high latitudes, and the low degree of hemispheric coupling.

The second important result came from Augustson et al. (2015) utilizing the 3D MHD ASH code which is shown in Fig. 23. This is from a model of one solar mass rotating at three times the Sun. Again this simulation produces many features that are consistent with observation and the important one is the equatorward migration of the toroidal field belt at low latitudes which is caused by the nonlinear modulation of the differential rotation. The interesting feature in their simulation is that a clear grand minimum was identified with a considerably reduced magnetic field for about five cycles. However during this minimum, the large-scale field failed to reverse, although its amplitude oscillated cyclically. The grand minimum in this simulation is possibly caused by the interplay between the symmetric and anti-symmetric dynamo families. During the regular cycle, the anti-symmetric dynamo family is greater than the symmetric family but during grand minimum phase, the symmetric family dominates over the anti-symmetric one; see the right panel of Fig. 23 for the increased parity of the radial field at two different depths. The mechanism for the generation of the grand minimum in this simulation is similar to the one proposed by Tobias (1997) and Moss and Brooke (2000) based on the nonlinear mean-field dynamo model.

The final one is from Käpylä et al. (2016) utilizing the Pencil Code. They performed this simulation for a model of one solar mass rotating at five times the Sun. This simulation also produced some solar-like features, including regular polarity reversals and an equatorward migration of the toroidal field at low latitudes (due to a nonlinear dynamo wave). In addition to the dominant global magnetic cycle of an average period of 4.9 years, there are two other prominent cycles, one having a higher frequency mode near the surface and at low latitudes with poleward migration, and the other one having low frequency residing at the BCZ. Their simulation also finds an episode of reduced magnetic field for about three cycles, happening asynchronously in hemispheres ($t = 20$–45 years). Interestingly, the magnetic field in the deeper CZ is stronger during this period and thus the global magnetic field during this period is larger than during the normal phase. The dynamics of the magnetic

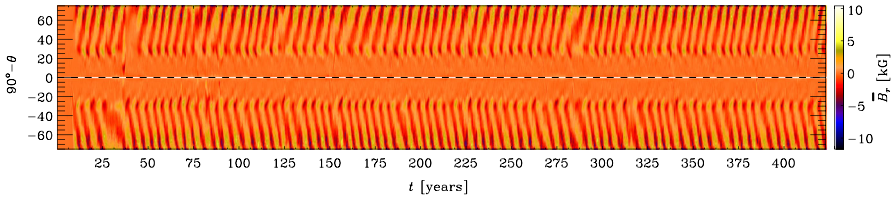

Fig. 24 Temporal variation of the mean B_r average over the longitudes on the surface from global convection simulation using Pencil Code (Käpylä et al. 2016). The color scale is saturated at the half of the extrema i.e., at [−11.7, 10.4] kG. Note the disturbed magnetic activity during $t = 20$–45 years. Image reproduced with permission from Käpylä et al. (2016), copyright by ESO

fields in this simulation are extremely complex and the grand episode of the reduced activity is caused through the interplay of various dynamo modes.

Although the global convection simulations produce some long-term modulations in the cycles and the grand minimum-like reduced activity which are consistent with solar observations, there are few caveats that we should keep in mind. The cycle modulations observed in the above convection simulations are many ways far from the actual Sun. The large-scale flows produced in these simulations are also quite far from the real Sun. Importantly, the power in the sub-surface convective flow at large scales are much stronger than that is obtained from the measurements, so-called the convective conundrum (Hanasoge et al. 2012; Lord et al. 2014; also see e.g., Hotta et al. 2015; Karak et al. 2018b for the studies that attempt to resolve this.) Furthermore, we do not have any information about whether these long-term modulations found in the convection simulations are robust in the model parameter regimes. Finally, the simulations do not produce BMRs which are important component of the solar cycle and are responsible for the generation of the poloidal field in the Sun, at least the field that is observed on the surface. Therefore, future work is needed to make the global convection simulations more realistic so that they can be utilized to study the long-term cycle modulation.

Ideal MHD simulations in the local box are also performed to study the large-scale dynamos. With helical forcing and imposed shear, Karak et al. (2015b) performed HMD simulations in the local Cartesian geometry and found modulations in the large-scale magnetic cycle. The interesting fact about their study was that they found grand minima like intermittent activity only when the dynamo operates in the subcritical and critical regime but not in the supercritical regime. This independent study thus supports the idea that the variability and the grand minima are less probable in the supercritical dynamo; see Sect. 6.2.5 for details. Local simulations are also useful to study the cycle modulations in presence of the small-scale dynamo. The small-scale magnetic field generated from the small-scale dynamo affects the flows and thus the global dynamo (Karak and Brandenburg 2016). Global dynamos are usually performed at low Reynolds numbers and thus small-scale dynamo is not excited, except a few (e.g., Nelson et al. 2013; Käpylä et al. 2017; Hotta and Kusano 2021), however, they are not ran for many cycles.

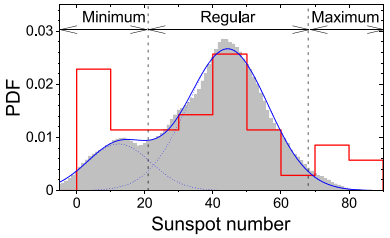

Fig. 25 Probability distribution function of the reconstructed sunspot number (filled grey curve) and the observed group sunspot number (red curve). Blue is the bi-Gaussian curve. Figure is modified after Usoskin et al. (2014); also see Wu et al. (2018) for the distribution from longer data

8 Some open questions and current trends

8.1 Do grand minima represent different states of the solar dynamo?

By analyzing the solar activity data for the past, Usoskin et al. (2014) showed that the distribution of the solar activity is bi-modal. Of this, the dominant mode corresponds to the regular activity phase and the reduced-activity mode which corresponds to the grand minima is distinct from the dominant regular one. As seen from Fig. 25, the distribution is clearly bimodal.

In terms of the dynamo theory, of course, the physics during grand minima is not quite the same as that during the regular cycle. For example, during the grand minima phases, the magnetic field falls to a low value and then the Sun takes some time to grow its magnetic field to the normal level. During these grand minima phases, the generation of the poloidal field is low because the Babcock–Leighton process which is the dominant source for the poloidal field in the Sun becomes less efficient due to fewer BMRs (Sect. 6.2.4). The strength and morphology of the flow can also be different during this phase. Therefore, the Babcock–Leighton dynamo models coupled with weak α-effect and/or the dynamo models coupled with the dynamic α-effect produced by the instability of flux tube (discussed in Sect. 6.2.2) can naturally explain the bimodal distribution. The dominant source of the poloidal field (Babcock–Leighton process or dynamic α-effect) maintains the normal mode of the solar activity while the grand minima phase is maintained by the weak α-effect. Time-delay models or the iterative map with low-amplitude additive noise and fluctuating map parameter/dynamo number with specific nonlinearity can also naturally produce the bimodal distribution of solar activity; see Fig. 1 of Charbonneau (2001) and Tripathi et al. (2021). Also, see Petrovay (2007) for a possible explanation of a bimodal solar dynamo based on an interface dynamo model coupled with a fast tachocline model. Karak et al. (2015b) using 3D simulations of turbulent dynamo suggested that the bimodal distribution of solar activity can be produced in the subcritical dynamo.

8.2 Do grand maxima require different mechanisms for their origin?

In most of the previous studies, the origin of the grand maxima is ignored. However, the mechanism for its generation is subtle because the dynamo is more nonlinear during the grand maxima phase. When the Sun tries to produce a strong magnetic field, the nonlinearity tries to quench its generation process (efficiencies of both the poloidal and toroidal field generations are reduced with magnetic field). Incidentally, the Sun spent less time in the grand maxima phase than in the grand minima phase (Usoskin et al. 2007; Solanki et al. 2004). Thus, producing extended grand maxima using the stochastic fluctuations in the dynamo parameters is less obvious. However, stochastic fluctuations still can produce a very strong magnetic cycles and grand maxima if they occur in a certain phase of the cycle. Kitchatinov and Olemskoy (2016) showed that at the beginning of a cycle (when the field at the poles is strongest) if the generation of the poloidal field is reversed (say due to the emergence of some wrongly tilted BMRs), then it will produce the same polarity field as it was there in the pole. Consequently, instead of reversing the old polarity polar field, it will amplify. This strong polar field will make the current cycle very strong. By introducing stochastic fluctuations in a 2D flux transport dynamo model, Kitchatinov and Olemskoy (2016) showed that this mechanism can occasionally produce a much stronger cycle which corresponds to the grand maxima phase. However, in this mechanism, not more than one strong cycle at a time is produced, while in the solar grand maximum, at least two consecutive cycles are strong (Usoskin et al. 2007). Also, this study is based on a kinematic model, in which the nonlinear feedback of the magnetic field on the flow is ignored.

Another way of generating the grand maxima is through the combined effect of multiple poloidal field generation processes. Ölçek et al. (2019) find that when the deep-seated α-effect is coupled with the surface Babcock–Leighton process in a dynamo model, these two processes more or less contribute equally to the generation of the poloidal field through a sort of constructive interference. This could be the mechanism of grand maxima in their dynamo model. However again this model is kinematic and the magnetic feedback is not taken care of.

8.3 What is the origin of Gnevyshev–Ohl/Even–Odd rule?

One plausible explanation for the Gnevyshev–Ohl rule is the fossil field hypothesis. A steady large-scale magnetic field of fossil origin (Boruta 1996) can interfere with the oscillating magnetic field from the CZ. In one cycle the oscillating magnetic field appears in the same polarity as that of the fossil field and it makes the cycle strong. In the next cycle, the oscillating magnetic field becomes of opposite polarity and thus the cycle becomes weak. To explain the Even–Odd rule using this idea, the fossil field has to be comparable to the dynamo-generated oscillating magnetic field at the BCZ which is of the order of 10 kG. However, the present observations do not confirm this strong fossil field. Furthermore, if the Gnevyshev–Ohl rule is caused by the fossil field, then there should be infinite memory in it, in a sense that once this rule is established, odd (even) cycles will always be stronger than the previous even (odd) cycles, even if there are some violations due to other effects. However, studies

show that there was a possible reversal in the even–odd pattern during 1745–1850 (Mursula et al. 2001; Tlatov 2013; Zolotova and Ponyavin 2015).

There is another possible explanation for the Gnevyshev–Ohl rule which was proposed by Durney (2000) using the nonlinear period-doubling effect. He suggested that the solar dynamo is operating in the region of period doubling beyond the bifurcation point and in this region the alternating amplitude modulation is unavoidable. Later Charbonneau (2001) showed that this is indeed not essential; stochastic forcing in the dynamo can lead to Even–Odd effect even outside this parameter range of period doubling. The time delays (Sect. 6.4) involved in the solar dynamo including simple amplitude limiting nonlinearity can produce the same period-doubling and Gnevyshev–Ohl rule as seen in the complex nonlinear system (Charbonneau et al. 2007). The dynamo model and map with various types of nonlinearity show Gnevyshev–Ohl rule under fluctuations in the poloidal source (α). However, this Gnevyshev–Ohl rule becomes evident only when the nonlinearity becomes important (large map parameter or dynamo number) and it seems to be little restricted to a narrow range of the diffusivity in the BCZ (Sec 4.5 of Charbonneau et al. 2005). Thus, there is still room to explore the robustness of this feature.

8.4 What are the causes of Gleissberg and Suess/de Vries cycles?

Gleissberg and Suess/de Vries cycles are not strictly cycles, rather they are modulation over the dominant 11-year period and they are detected in the cosmogenic data having ranges of periods from 90 to 100 years and from 205 to 210 years, respectively. If these modulations are the true nature of the solar cycle, then they are probably coming from the nonlinear interaction between the magnetic field and the flows in the lower part of CZ. In a axisymmetric $\alpha\Omega$ dynamo model coupled with the angular momentum equation and ignoring meridional circulation, Pipin (1999) showed that the Gleissberg cycle is a results from the magnetic feedback on the angular momentum fluxes which maintains the differential rotation in the CZ. In this model, the period of the Gleissberg cycle is determined by the time associated with the re-establishment of the differential rotation after the magnetic perturbations of the angular momentum transport. If this is the mechanism of the Gleissberg cycle in the sun, then the observed differential rotation should show a variation in the Gleissberg timescale. However, the available observations does not provide a conclusive evidence on it (Howard 1978). Passos and Charbonneau (2014) found a hint of Gleissberg modulation in their computed proxy sunspot number but not in the radial field data and they require data for a longer duration to confirm its existence. Cameron and Schüssler (2019) showed that Gleissberg and Suess/de Vries cycles are consistent with realization noise and the noisy normal form model can reproduce these modulations.

9 Summary and discussion

Besides the 11-year (a)periodic variation of the amplitude, the most prominent variation of the solar cycle is the long-term modulation which has been unambiguously identified in the direct and indirect (cosmogenic data) observations

of the solar activity. Examples of the long-term modulation include the Gnevyshev–Ohl/Even–Odd rule, grand minima, grand maxima, Gleissberg cycle and Suess cycles. In this review, we have presented comprehensive discussions on the origins and models of long-term variations. To do so, we have broadly identified the following three major causes for the cycle modulations: (1) magnetic feedback on the flow, (2) stochastic forcing, and (3) time delays in various dynamo processes. Problems in the nonlinear mean-field models are that not all possible nonlinearities are always included in the model and the resulting mean flows and magnetic fields are not compared carefully with observations. Global MHD convection simulations are very useful in this respect because all nonlinearities are captured by default. They have begun to produce some correct results of the large-scale field and the flow, however, there are big discrepancies as well. Until global convection simulations reach somewhat realistic parameter regimes and resolve the major issues (convective conundrum, observed large-scale flows, nonappearance of BMRs), we need to rely on the mean-field models only.

Stochastic fluctuations in the mean-field models are enough to explain many features of the long-term variabilities. The Babcock–Leighton dynamo models are promising models for the solar cycle, in terms of their success in reproducing the long-term modulations in the solar cycle. Stochastic fluctuations in these models are due to randomness in the BMR properties (primarily due to scatter around Joy's law, BMR emergence rates and emergence latitudes). Babcock–Leighton models are also nonlinear because at least the toroidal to poloidal field generation step includes several essential nonlinearities (tilt quenching, latitude quenching, toroidal flux loss due to magnetic buoyancy). While these nonlinearities have the tendency of stabilizing the magnetic field, they can lead to fluctuating cycles including Gnevyshev–Ohl rule and grand minima at highly supercritical regimes (large dynamo numbers) due to the inherent time delay in the dynamo models with spatially segregated source regions. Observations indicate that the solar dynamo is possibly operating in a weakly nonlinear regime (slightly above the dynamo transition) and thus cycle modulations are caused by stochastic effects.

One way to pick up the correct model out of all the possible models for long-term modulation is to carefully compare the model results with the observations. Observational results include the followings (but not limited to). (1) There is a strong hemispheric asymmetry during the second half of the Maunder Minimum (Ribes and Nesme-Ribes 1993). (2) However, the asymmetry during the normal cycle is less, appears randomly, and is smoothed out in a few cycles (the memory of the asymmetry does not remain for multiple cycles; Goel and Choudhuri 2009; McIntosh et al. 2013; Das et al. 2022). (3) The differential rotation in the whole CZ of the Sun is well-measured for about last four decades and it has only a tiny variation (surface differential is measured even for about 200 years and also shows little variation; Gilman and Howard 1984; Jha et al. 2021.)

Grand minima are possibly triggered by the stochastic fluctuations in the dynamo parameters or/and the nonlinear interaction of the Lorentz force. The recovery to the normal phase from grand minima is trivial in any model which includes the α-effect because it can operate in the weak-field regime. Recovery through the Babcock–Leighton process is also possible because recent analyses revealed spots during

Maunder minimum and the Babcock–Leighton process can produce a poloidal field with a few BMRs or smaller BMRs having nonzero tilts (including ephemeral regions). Grand maxima are probably more special events and less frequent than grand minima. Again nonlinear modulation of the flow via Lorentz force and stochastic fluctuations can trigger these events. A dual source of poloidal field generation occurring constructively or reversed generation of the poloidal field due to stochastic fluctuations can produce prominent grand maxima. Occurrences of grand minima and maxima in the dynamo models can be described by stochastic processes and these are consistent with the observations. The waiting time distributions of the grand minima and maxima in the dynamo models are also described by the memoryless stochastic processes, which however disagree with the available observations.

Acknowledgements Author shows gratitude to Akash Biswas, Bibhuti Kumar Jha, Leonid Kitchatinov, Paul Charbonneau, Pawan Kumar, and two (anonymous) brilliant referees for carefully reviewing and pointing out many mistakes in the earlier version of the draft. Author also thanks Pawan Kumar and Anu B Sreedevi for their help in preparing many figures. Ilya Usoskin, Leonid Kitchatinov, Jie Jiang, Alexandre Lemerle, Maarit Käpylä, Dibyendu Nandi, and Sacha Brun have kindly provided data and/or figures for this article. Author acknowledges financial support provided by ISRO/RESPOND (project No. ISRO/RES/2/430/19-20) and Ramanujan Fellowship (project no SB/S2/RJN-017/2018) and the computational resources of the PARAM Shivay Facility under the National Supercomputing Mission, the Government of India, at the Indian Institute of Technology Varanasi. SOHO is a project of international cooperation between ESA and NASA. Courtesy of NASA/SDO and the HMI science teams.

References

Albert C, Ferriz-Mas A, Gaia F, Ulzega S (2021) Can stochastic resonance explain recurrence of Grand Minima? Astrophys J Lett 916(2):L9. https://doi.org/10.3847/2041-8213/ac0fd6

Augustson K, Brun AS, Miesch M, Toomre J (2015) Grand minima and equatorward propagation in a cycling stellar convective dynamo. Astrophys J 809:149. https://doi.org/10.1088/0004-637X/809/2/149. arXiv:1410.6547 [astro-ph.SR]

Babcock HW (1961) The topology of the Sun's magnetic field and the 22-year cycle. Astrophys J 133:572. https://doi.org/10.1086/147060

Baliunas SL, Donahue RA, Soon WH, Horne JH, Frazer J, Woodard-Eklund L, Bradford M, Rao LM, Wilson OC, Zhang Q, Bennett W, Briggs J, Carroll SM, Duncan DK, Figueroa D, Lanning HH, Misch T, Mueller J, Noyes RW, Poppe D, Porter AC, Robinson CR, Russell J, Shelton JC, Soyumer T, Vaughan AH, Whitney JH (1995) Chromospheric variations in main-sequence stars. Astrophys J 438:269–287. https://doi.org/10.1086/175072

Barker DM, Moss D (1994) The nonlinear limitation of nonaxisymmetric mean field dynamos by the large scale Lorentz force. Astron Astrophys 283:1009

Baum AC, Wright JT, Luhn JK, Isaacson H (2022) Five decades of chromospheric activity in 59 Sun-like stars and new Maunder Minimum candidate HD 166620. Astron J 163(4):183. https://doi.org/10.3847/1538-3881/ac5683. arXiv:2203.13376 [astro-ph.SR]

Baumann I, Schmitt D, Schüssler M, Solanki SK (2004) Evolution of the large-scale magnetic field on the solar surface: a parameter study. Astron Astrophys 426:1075–1091. https://doi.org/10.1051/0004-6361:20048024

Beer J, Tobias S, Weiss N (1998) An active Sun throughout the Maunder minimum. Sol Phys 181:237–249. https://doi.org/10.1023/A:1005026001784

Beer J, Tobias SM, Weiss NO (2018) On long-term modulation of the Sun's magnetic cycle. Mon Not R Astron Soc 473(2):1596–1602. https://doi.org/10.1093/mnras/stx2337

Bekki Y, Cameron R (2022) Three-dimensional non-kinematic simulation of post-emergence evolution of bipolar magnetic regions and Babcock-Leighton dynamo of the Sun. Astron Astrophys (submitted). https://doi.org/10.1051/0004-6361/201322635

Biswas A, Karak BB, Cameron R (2022) Toroidal flux loss due to flux emergence explains why solar cycles rise differently but decay in a similar way. Phys Rev Lett 129(24):241102. https://doi.org/10.1103/PhysRevLett.129.241102. arXiv:2210.07061 [astro-ph.SR]

Biswas A, Karak BB, Usoskin I, Weisshaar E (2023) Long-term modulation of solar cycles. Space Sci Rev 219(3):19. https://doi.org/10.1007/s11214-023-00968-w. arXiv:2302.14845 [astro-ph.SR]

Boro Saikia S, Marvin CJ, Jeffers SV, Reiners A, Cameron R, Marsden SC, Petit P, Warnecke J, Yadav AP (2018) Chromospheric activity catalogue of 4454 cool stars. Questioning the active branch of stellar activity cycles. Astron Astrophys 616:A108. https://doi.org/10.1051/0004-6361/201629518. arXiv:1803.11123 [astro-ph.SR]

Boruta N (1996) Solar dynamo surface waves in the presence of a primordial magnetic field: a 30 gauss upper limit in the solar core. Astrophys J 458:832. https://doi.org/10.1086/176861

Brandenburg A, Spiegel EA (2008) Modeling a Maunder minimum. Astron Nachr 329:351

Brandenburg A, Subramanian K (2005) Astrophysical magnetic fields and nonlinear dynamo theory. Phys Rep Rep 417:1–209. https://doi.org/10.1016/j.PhysRep.2005.06.005.astro-ph/0405052

Brandenburg A, Krause F, Meinel R, Moss D, Tuominen I (1989) The stability of nonlinear dynamos and the limited role of kinematic growth rates. Astron Astrophys 213:411–422

Brandenburg A, Moss D, Rüdiger G, Tuominen I (1991) Hydromagnetic αΩ-type dynamos with feedback from large scale motions. Geophys Astrophys Fluid Dyn 61(1):179–198. https://doi.org/10.1080/03091929108229043

Brandenburg A, Rädler KH, Rheinhardt M, Käpylä PJ (2008) Magnetic diffusivity tensor and dynamo effects in rotating and shearing turbulence. Astrophys J 676(1):740–751. https://doi.org/10.1086/527373. arXiv:0710.4059 [astro-ph]

Bushby PJ (2006) Zonal flows and grand minima in a solar dynamo model. Mon Not R Astron Soc 371(2):772–780. https://doi.org/10.1111/j.1365-2966.2006.10706.x

Cameron RH, Schüssler M (2012) Are the strengths of solar cycles determined by converging flows towards the activity belts? Astron Astrophys 548:A57. https://doi.org/10.1051/0004-6361/201219914. arXiv:1210.7644 [astro-ph.SR]

Cameron R, Schüssler M (2015) The crucial role of surface magnetic fields for the solar dynamo. Science 347:1333–1335. https://doi.org/10.1126/science.1261470. arXiv:1503.08469 [astro-ph.SR]

Cameron RH, Schüssler M (2016) The turbulent diffusion of toroidal magnetic flux as inferred from properties of the sunspot butterfly diagram. Astron Astrophys 591:A46. https://doi.org/10.1051/0004-6361/201527284. arXiv:1604.07340 [astro-ph.SR]

Cameron RH, Schüssler M (2017) Understanding solar cycle variability. Astrophys J 843(2):111. https://doi.org/10.3847/1538-4357/aa767a. arXiv:1705.10746 [astro-ph.SR]

Cameron RH, Schüssler M (2019) Solar activity: periodicities beyond 11 years are consistent with random forcing. Astron Astrophys 625:A28. https://doi.org/10.1051/0004-6361/201935290

Cameron RH, Schmitt D, Jiang J, Işık E (2012) Surface flux evolution constraints for flux transport dynamos. Astron Astrophys 542:A127. https://doi.org/10.1051/0004-6361/201218906. arXiv:1205.1136 [astro-ph.SR]

Cameron RH, Dasi-Espuig M, Jiang J, Işık E, Schmitt D, Schüssler M (2013) Limits to solar cycle predictability: cross-equatorial flux plumes. Astron Astrophys 557:A141. https://doi.org/10.1051/0004-6361/201321981. arXiv:1308.2827 [astro-ph.SR]

Chakraborty S, Choudhuri AR, Chatterjee P (2009) Why does the Sun's torsional oscillation begin before the sunspot cycle? Phys Rev Lett 102(4):041102. https://doi.org/10.1103/PhysRevLett.102.041102. arXiv:0907.4842 [astro-ph.SR]

Charbonneau P (2001) Multiperiodicity, Chaos, and intermittency in a reduced model of the solar cycle. Sol Phys 199(2):385–404. https://doi.org/10.1023/A:1010387509792
Charbonneau P (2005) A Maunder minimum scenario based on cross-hemispheric coupling and intermittency. Sol Phys 229(2):345–358. https://doi.org/10.1007/s11207-005-8150-0
Charbonneau P (2010) Dynamo models of the solar cycle. Living Rev Sol Phys 7:3. https://doi.org/10.12942/lrsp-2010-3
Charbonneau P (2020) Dynamo models of the solar cycle. Living Rev Sol Phys 17:4. https://doi.org/10.1007/s41116-020-00025-6
Charbonneau P, Dikpati M (2000) Stochastic fluctuations in a Babcock–Leighton model of the solar cycle. Astrophys J 543:1027–1043. https://doi.org/10.1086/317142
Charbonneau P, Blais-Laurier G, St-Jean C (2004) Intermittency and phase persistence in a Babcock–Leighton model of the solar cycle. Astrophys J Lett 616:L183–L186. https://doi.org/10.1086/426897
Charbonneau P, St-Jean C, Zacharias P (2005) Fluctuations in Babcock–Leighton dynamos. I. Period doubling and transition to chaos. Astrophys J 619(1):613–622. https://doi.org/10.1086/426385
Charbonneau P, Beaubien G, St-Jean C (2007) Fluctuations in Babcock–Leighton dynamos. II. Revisiting the Gnevyshev–Ohl rule. Astrophys J 658(1):657–662. https://doi.org/10.1086/511177
Chatterjee P, Choudhuri AR (2006) On magnetic coupling between the two hemispheres in solar dynamo models. Sol Phys 239(1–2):29–39. https://doi.org/10.1007/s11207-006-0201-6
Chatterjee P, Nandy D, Choudhuri AR (2004) Full-sphere simulations of a circulation-dominated solar dynamo: exploring the parity issue. Astron Astrophys 427:1019–1030. https://doi.org/10.1051/0004-6361:20041199.astro-ph/0405027
Chatterjee P, Mitra D, Rheinhardt M, Brandenburg A (2011) Alpha effect due to buoyancy instability of a magnetic layer. Astron Astrophys 534:A46. https://doi.org/10.1051/0004-6361/201016108. arXiv:1011.1218 [astro-ph.SR]
Choudhuri AR (1992) Stochastic fluctuations of the solar dynamo. Astron Astrophys 253:277–285
Choudhuri AR, Karak BB (2009) A possible explanation of the Maunder minimum from a flux transport dynamo model. Res Astron Astrophys 9:953–958. https://doi.org/10.1088/1674-4527/9/9/001. arXiv:0907.3106 [astro-ph.SR]
Choudhuri AR, Karak BB (2012) Origin of grand minima in sunspot cycles. Phys Rev Lett 109 (17):171103
Choudhuri AR, Schüssler M, Dikpati M (1995) The solar dynamo with meridional circulation. Astron Astrophys 303:L29
Das R, Ghosh A, Karak BB (2022) Is the hemispheric asymmetry of sunspot cycle caused by an irregular process with long-term memory? Mon Not R Astron Soc 551:472. https://doi.org/10.1093/mnras/stac035
Dasi-Espuig M, Solanki SK, Krivova NA, Cameron R, Peñuela T (2010) Sunspot group tilt angles and the strength of the solar cycle. Astron Astrophys 518:A7. https://doi.org/10.1051/0004-6361/201014301. arXiv:1005.1774 [astro-ph.SR]
Dasi-Espuig M, Solanki SK, Krivova NA, Cameron R, Peñuela T (2013) Sunspot group tilt angles and the strength of the solar cycle (Corrigendum). Astron Astrophys 556:C3. https://doi.org/10.1051/0004-6361/201014301e
Dikpati M, Charbonneau P (1999) A Babcock–Leighton flux transport dynamo with solar-like differential rotation. Astrophys J 518:508–520. https://doi.org/10.1086/307269
D'Silva S, Choudhuri AR (1993) A theoretical model for tilts of bipolar magnetic regions. Astron Astrophys 272:621
Durney BR (1995) On a Babcock–Leighton dynamo model with a deep-seated generating layer for the toroidal magnetic field. Sol Phys 160:213–235. https://doi.org/10.1007/BF00732805
Durney BR (2000) On the differences between odd and even solar cycles. Sol Phys 196(2):421–426. https://doi.org/10.1023/A:1005285315323
Eddy JA (1976) The Maunder minimum. Science 192:1189–1202. https://doi.org/10.1126/science.192.4245.1189
Fan Y (2021) Magnetic fields in the solar convection zone. Living Rev Sol Phys 6:4. https://doi.org/10.12942/lrsp-2009-4
Fan Y, Fang F (2014) A simulation of convective dynamo in the solar convective envelope: maintenance of the solar-like differential rotation and emerging flux. Astrophys J 789:35. https://doi.org/10.1088/0004-637X/789/1/35. arXiv:1405.3926 [astro-ph.SR]
Fan Y, Fisher GH, McClymont AN (1994) Dynamics of emerging active region flux loops. Astrophys J 436:907–928. https://doi.org/10.1086/174967

Field GB, Blackman EG (2002) Dynamical quenching of the α^2 dynamo. Astrophys J 572(1):685–692. https://doi.org/10.1086/340233. arXiv:astro-ph/0111470 [astro-ph]
Forgács-Dajka E, Major B, Borkovits T (2004) Long-term variation in distribution of sunspot groups. Astron Astrophys 424:311–315. https://doi.org/10.1051/0004-6361:20040550. arXiv:astro-ph/0606053 [astro-ph]
Fournier Y, Arlt R, Elstner D (2018) Delayed Babcock–Leighton dynamos in the diffusion-dominated regime. Astron Astrophys 620:A135. https://doi.org/10.1051/0004-6361/201834131. arXiv:1808.08135 [astro-ph.SR]
Garg S, Karak BB, Egeland R, Soon W, Baliunas S (2019) Waldmeier effect in stellar cycles. Astrophys J 886(2):132. https://doi.org/10.3847/1538-4357/ab4a17. arXiv:1909.12148 [astro-ph.SR]
Getling AV, Buchnev AA (2019) The origin and early evolution of a bipolar magnetic region in the solar photosphere. Astrophys J 871(2):224. https://doi.org/10.3847/1538-4357/aafad9. arXiv:1805.06486 [astro-ph.SR]
Gilman PA (1983) Dynamically consistent nonlinear dynamos driven by convection in a rotating spherical shell. II. Dynamos with cycles and strong feedbacks. Astrophys J Suppl 53:243–268. https://doi.org/10.1086/190891
Gilman PA, Howard R (1984) Variations in solar rotation with the sunspot cycle. Astrophys J 283:385–391. https://doi.org/10.1086/162316
Gizon L, Rempel M (2008) Observation and modeling of the solar-cycle variation of the meridional flow. Sol Phys 251(1–2):241–250. https://doi.org/10.1007/s11207-008-9162-3. arXiv:0803.0950 [astro-ph]
Gizon L, Duvall JTL, Larsen RM (2001) Probing surface flows and magnetic activity with time-distance helioseismology. In: Brekke P, Fleck B, Gurman JB (eds) Recent insights into the physics of the Sun and heliosphere: highlights from SOHO and other space missions. IAU symposium, vol 203. Astronomical Society of the Pacific, San Francisco, p 189
Gizon L, Cameron RH, Pourabdian M, Liang ZC, Fournier D, Birch AC, Hanson CS (2020) Meridional flow in the Sun's convection zone is a single cell in each hemisphere. Science 368(6498):1469–1472. https://doi.org/10.1126/science.aaz7119
Glatzmaier GA (1984) Numerical simulations of stellar convective dynamos. I. The model and method. J Comput Phys 55:461–484. https://doi.org/10.1016/0021-9991(84)90033-0
Glatzmaier GA (1985) Numerical simulations of stellar convective dynamos. II. Field propagation in the convection zone. Astrophys J 291:300–307. https://doi.org/10.1086/163069
Gleissberg W (1939) A long-periodic fluctuation of the sun-spot numbers. Observatory 62:158–159
Gnevyshev MN, Ohl A (1948) On the 22-year cycle of solar activity. Astron Zh 25:18
Goel A, Choudhuri AR (2009) The hemispheric asymmetry of solar activity during the last century and the solar dynamo. Res Astron Astrophys 9:115–126. https://doi.org/10.1088/1674-4527/9/1/010. arXiv:0712.3988
Gómez DO, Mininni PD (2006) Description of Maunder-like events from a stochastic alpha omega model. Adv Space Res 38(5):856–861. https://doi.org/10.1016/j.asr.2005.07.032
González Hernández I, Komm R, Hill F, Howe R, Corbard T, Haber DA (2006) Meridional circulation variability from large-aperture ring-diagram analysis of global oscillation network group and Michelson doppler imager data. Astrophys J 638(1):576–583. https://doi.org/10.1086/498642
González Hernández I, Kholikov S, Hill F, Howe R, Komm R (2008) Subsurface meridional circulation in the active belts. Sol Phys 252(2):235–245. https://doi.org/10.1007/s11207-008-9264-y. arXiv:0808.3606 [astro-ph]
González Hernández I, Howe R, Komm R, Hill F (2010) Meridional circulation during the extended solar minimum: another component of the torsional oscillation? Astrophys J Lett 713(1):L16–L20. https://doi.org/10.1088/2041-8205/713/1/L16. arXiv:1003.1685 [astro-ph.SR]
Guerrero G, de Gouveia Dal Pino EM (2008) Turbulent magnetic pumping in a Babcock–Leighton solar dynamo model. Astron Astrophys 485:267–273. https://doi.org/10.1051/0004-6361:200809351. arXiv:0803.3466
Hagenaar HJ, Schrijver CJ, Title AM (2003) The properties of small magnetic regions on the solar surface and the implications for the solar dynamo(s). Astrophys J 584:1107–1119. https://doi.org/10.1086/345792
Hale GE, Ellerman F, Nicholson SB, Joy AH (1919) The magnetic polarity of sun-spots. Astrophys J 49:153. https://doi.org/10.1086/142452

Hanasoge SM, Duvall TL, Sreenivasan KR (2012) Anomalously weak solar convection. Proc Natl Acad Sci USA 109:11928–11932. https://doi.org/10.1073/pnas.1206570109. arXiv:1206.3173 [astro-ph.SR]

Hathaway DH (2015) The solar cycle. Living Rev Sol Phys 12:4. https://doi.org/10.1007/lrsp-2015-4. arXiv:1502.07020 [astro-ph.SR]

Hathaway DH, Rightmire L (2010) Variations in the Sun's meridional flow over a solar cycle. Science 327 (5971):1350. https://doi.org/10.1126/science.1181990

Hazra G, Choudhuri AR (2017) A theoretical model of the variation of the meridional circulation with the solar cycle. Mon Not R Astron Soc 472(3):2728–2741. https://doi.org/10.1093/mnras/stx2152. arXiv:1708.05204 [astro-ph.SR]

Hazra S, Nandy D (2019) The origin of parity changes in the solar cycle. Mon Not R Astron Soc 489 (3):4329–4337. https://doi.org/10.1093/mnras/stz2476. arXiv:1906.06780 [astro-ph.SR]

Hazra G, Karak BB, Choudhuri AR (2014) Is a deep one-cell meridional circulation essential for the flux transport solar dynamo? Astrophys J 782:93. https://doi.org/10.1088/0004-637X/782/2/93. arXiv:1309.2838 [astro-ph.SR]

Hazra G, Karak BB, Banerjee D, Choudhuri AR (2015) Correlation between decay rate and amplitude of solar cycles as revealed from observations and dynamo theory. Sol Phys 290:1851–1870. https://doi.org/10.1007/s11207-015-0718-8. arXiv:1410.8641 [astro-ph.SR]

Hazra G, Choudhuri AR, Miesch MS (2017) A theoretical study of the build-up of the Sun polar magnetic field by using a 3d kinematic dynamo model. Astrophys J 835:39. https://doi.org/10.3847/1538-4357/835/1/39. arXiv:1610.02726 [astro-ph.SR]

Hazra S, Passos D, Nandy D (2014) A stochastically forced time delay solar dynamo model: self-consistent recovery from a Maunder-like grand minimum necessitates a mean-field alpha effect. Astrophys J 789:5. https://doi.org/10.1088/0004-637X/789/1/5. arXiv:1307.5751 [astro-ph.SR]

Hotta H, Kusano K (2021) Solar differential rotation reproduced with high-resolution simulation. Nat Astron 5:1100–1102. https://doi.org/10.1038/s41550-021-01459-0. arXiv:2109.06280 [astro-ph.SR]

Hotta H, Rempel M, Yokoyama T (2015) Efficient small-scale dynamo in the solar convection zone. Astrophys J 803:42. https://doi.org/10.1088/0004-637X/803/1/42. arXiv:1502.03846 [astro-ph.SR]

Howard R (1978) The rotation of the Sun. Rev Geophys Space Phys 16:721–732. https://doi.org/10.1029/RG016i004p00721

Howard RF (1991) Axial tilt angles of sunspot groups. Sol Phys 136:251–262. https://doi.org/10.1007/BF00146534

Howe R (2009) Solar interior rotation and its variation. Living Rev Sol Phys 6:1. https://doi.org/10.12942/lrsp-2009-1. arXiv:0902.2406 [astro-ph.SR]

Hoyng P (1988) Turbulent transport of magnetic fields. III. Stochastic excitation of global magnetic modes. Astrophys J 332:857–871

Hoyng P (1993) Helicity fluctuations in mean field theory: an explanation for the variability of the solar cycle? Astron Astrophys 272:321

Hoyt DV, Schatten KH (1996) How well was the Sun observed during the Maunder minimum? Sol Phys 165:181–192

Hung CP, Jouve L, Brun AS, Fournier A, Talagrand O (2015) Estimating the deep solar meridional circulation using magnetic observations and a dynamo model: a variational approach. Astrophys J 814(2):151. https://doi.org/10.1088/0004-637X/814/2/151. arXiv:1710.02084 [astro-ph.SR]

Hung CP, Brun AS, Fournier A, Jouve L, Talagrand O, Zakari M (2017) Variational estimation of the large-scale time-dependent meridional circulation in the Sun: proofs of concept with a solar mean field dynamo model. Astrophys J 849(2):160. https://doi.org/10.3847/1538-4357/aa91d1. arXiv:1710.02114 [astro-ph.SR]

Inceoglu F, Arlt R, Rempel M (2017) The nature of grand minima and maxima from fully nonlinear flux transport dynamos. Astrophys J 848(2):93. https://doi.org/10.3847/1538-4357/aa8d68. arXiv:1710.08644 [astro-ph.SR]

Jennings RL (1993) A nonlinear model of the solar dynamo. Sol Phys 143(1):1–17. https://doi.org/10.1007/BF00619093

Jha BK, Karak BB, Mandal S, Banerjee D (2020) Magnetic field dependence of bipolar magnetic region tilts on the Sun: indication of tilt quenching. Astrophys J Lett 889(1):L19. https://doi.org/10.3847/2041-8213/ab665c. arXiv:1912.13223 [astro-ph.SR]

Jha BK, Priyadarshi A, Mandal S, Chatterjee S, Banerjee D (2021) Measurements of solar differential rotation using the century long Kodaikanal sunspot data. Sol Phys 296(1):25. https://doi.org/10.1007/s11207-021-01767-8. arXiv:2101.01941 [astro-ph.SR]

Jiang J (2020) Nonlinear mechanisms that regulate the solar cycle amplitude. Astrophys J 900(1):19. https://doi.org/10.3847/1538-4357/abaa4b. arXiv:2007.07069 [astro-ph.SR]
Jiang J, Işik E, Cameron RH, Schmitt D, Schüssler M (2010) The effect of activity-related meridional flow modulation on the strength of the solar polar magnetic field. Astrophys J 717(1):597–602. https://doi.org/10.1088/0004-637X/717/1/597. arXiv:1005.5317 [astro-ph.SR]
Jiang J, Cameron RH, Schüssler M (2014) Effects of the scatter in sunspot group tilt angles on the large-scale magnetic field at the solar surface. Astrophys J 791:5. https://doi.org/10.1088/0004-637X/791/1/5. arXiv:1406.5564 [astro-ph.SR]
Jiang J, Hathaway DH, Cameron RH, Solanki SK, Gizon L, Upton L (2014) Magnetic flux transport at the solar surface. Space Sci Rev 186:491–523. https://doi.org/10.1007/s11214-014-0083-1. arXiv:1408.3186 [astro-ph.SR]
Jiao Q, Jiang J, Wang ZF (2021) Sunspot tilt angles revisited: dependence on the solar cycle strength. Astron Astrophys 653:A27. https://doi.org/10.1051/0004-6361/202141215. arXiv:2106.11615 [astro-ph.SR]
Jouve L, Proctor MRE, Lesur G (2010) Buoyancy-induced time delays in Babcock–Leighton flux-transport dynamo models. Astron Astrophys 519:A68. https://doi.org/10.1051/0004-6361/201014455. arXiv:1005.2283 [astro-ph.SR]
Käpylä MJ, Käpylä PJ, Olspert N, Brandenburg A, Warnecke J, Karak BB, Pelt J (2016) Multiple dynamo modes as a mechanism for long-term solar activity variations. Astron Astrophys 589:A56. https://doi.org/10.1051/0004-6361/201527002. arXiv:1507.05417 [astro-ph.SR]
Käpylä PJ (2019) Effects of small-scale dynamo and compressibility on the Λ effect. Astron Nachr 340(8):744–751. https://doi.org/10.1002/asna.201913632. arXiv:1903.04363 [astro-ph.SR]
Käpylä PJ, Brandenburg A (2009) Turbulent dynamos with shear and fractional helicity. Astrophys J 699:1059–1066. https://doi.org/10.1088/0004-637X/699/2/1059. arXiv:0810.2298
Käpylä PJ, Käpylä MJ, Olspert N, Warnecke J, Brandenburg A (2017) Convection-driven spherical shell dynamos at varying Prandtl numbers. Astron Astrophys 599:A4. https://doi.org/10.1051/0004-6361/201628973. arXiv:1605.05885 [astro-ph.SR]
Käpylä PJ, Gent FA, Olspert N, Käpylä MJ, Brandenburg A (2020) Sensitivity to luminosity, centrifugal force, and boundary conditions in spherical shell convection. Geophys Astrophys Fluid Dyn 114(1–2):8–34. https://doi.org/10.1080/03091929.2019.1571586. arXiv:1807.09309 [astro-ph.SR]
Karak BB (2010) Importance of meridional circulation in flux transport dynamo: the possibility of a Maunder-like grand minimum. Astrophys J 724:1021–1029. https://doi.org/10.1088/0004-637X/724/2/1021. arXiv:1009.2479 [astro-ph.SR]
Karak BB (2020) Dynamo saturation through the latitudinal variation of bipolar magnetic regions in the Sun. Astrophys J Lett 901(2):L35. https://doi.org/10.3847/2041-8213/abb93f. arXiv:2009.06969 [astro-ph.SR]
Karak BB, Brandenburg A (2016) Is the small-scale magnetic field correlated with the dynamo cycle? Astrophys J 816(1):28. https://doi.org/10.3847/0004-637X/816/1/28. arXiv:1505.06632 [astro-ph.SR]
Karak BB, Cameron R (2016) Babcock–Leighton solar dynamo: the role of downward pumping and the equatorward propagation of activity. Astrophys J 832:94. https://doi.org/10.3847/0004-637X/832/1/94. arXiv:1605.06224 [astro-ph.SR]
Karak BB, Choudhuri AR (2011) The Waldmeier effect and the flux transport solar dynamo. Mon Not R Astron Soc 410:1503–1512. https://doi.org/10.1111/j.1365-2966.2010.17531.x. arXiv:1008.0824 [astro-ph.SR]
Karak BB, Choudhuri AR (2012) Quenching of meridional circulation in flux transport dynamo models. Sol Phys 278:137–148. https://doi.org/10.1007/s11207-012-9928-5. arXiv:1111.1540 [astro-ph.SR]
Karak BB, Choudhuri AR (2013) Studies of grand minima in sunspot cycles by using a flux transport solar dynamo model. Res Astron Astrophys 13:1339. https://doi.org/10.1088/1674-4527/13/11/005. arXiv:1306.5438 [astro-ph.SR]
Karak BB, Miesch M (2017) Solar cycle variability induced by tilt angle scatter in a Babcock–Leighton solar dynamo model. Astrophys J 847:69. https://doi.org/10.3847/1538-4357/aa8636. arXiv:1706.08933 [astro-ph.SR]
Karak BB, Miesch M (2018) Recovery from Maunder-like grand minima in a Babcock–Leighton solar dynamo model. Astrophys J Lett 860:L26. https://doi.org/10.3847/2041-8213/aaca97. arXiv:1712.10130 [astro-ph.SR]

Karak BB, Nandy D (2012) Turbulent pumping of magnetic flux reduces solar cycle memory and thus impacts predictability of the Sun's activity. Astrophys J Lett 761:L13. https://doi.org/10.1088/2041-8205/761/1/L13. arXiv:1206.2106 [astro-ph.SR]

Karak BB, Jiang J, Miesch MS, Charbonneau P, Choudhuri AR (2014) Flux transport dynamos: from kinematics to dynamics. Space Sci Rev 186:561–602. https://doi.org/10.1007/s11214-014-0099-6

Karak BB, Rheinhardt M, Brandenburg A, Käpylä PJ, Käpylä MJ (2014) Quenching and anisotropy of hydromagnetic turbulent transport. Astrophys J 795:16. https://doi.org/10.1088/0004-637X/795/1/16. arXiv:1406.4521 [astro-ph.SR]

Karak BB, Käpylä PJ, Käpylä MJ, Brandenburg A, Olspert N, Pelt J (2015a) Magnetically controlled stellar differential rotation near the transition from solar to anti-solar profiles. Astron Astrophys 576: A26. https://doi.org/10.1051/0004-6361/201424521. arXiv:1407.0984 [astro-ph.SR]

Karak BB, Kitchatinov LL, Brandenburg A (2015b) Hysteresis between distinct modes of turbulent dynamos. Astrophys J 803:95. https://doi.org/10.1088/0004-637X/803/2/95. arXiv:1411.0485 [astro-ph.SR]

Karak BB, Mandal S, Banerjee D (2018a) Double peaks of the solar cycle: an explanation from a dynamo model. Astrophys J 866(1):17. https://doi.org/10.3847/1538-4357/aada0d. arXiv:1808.03922 [astro-ph.SR]

Karak BB, Miesch M, Bekki Y (2018b) Consequences of high effective Prandtl number on solar differential rotation and convective velocity. Phys Fluids 30(4):046602. https://doi.org/10.1063/1.5022034. arXiv:1801.00560 [astro-ph.SR]

Kichatinov LL, Rüdiger G (1993) Λ-effect and differential rotation in stellar convection zones. Astron Astrophys 276:96–102

Kippenhahn R (1963) Differential rotation in stars with convective envelopes. Astrophys J 137:664. https://doi.org/10.1086/147539

Kitchatinov L, Nepomnyashchikh A (2017) How supercritical are stellar dynamos, or why do old main-sequence dwarfs not obey gyrochronology? Mon Not R Astron Soc 470(3):3124–3130. https://doi.org/10.1093/mnras/stx1473. arXiv:1706.02814 [astro-ph.SR]

Kitchatinov LL, Olemskoy SV (2010) Dynamo hysteresis and grand minima of solar activity. Astron Lett 36:292–296

Kitchatinov LL, Olemskoy SV (2011a) Alleviation of catastrophic quenching in solar dynamo model with nonlocal alpha-effect. Astron Nachr 332(5):496. https://doi.org/10.1002/asna.201011549. arXiv:1101.3115 [astro-ph.SR]

Kitchatinov LL, Olemskoy SV (2011b) Does the Babcock–Leighton mechanism operate on the Sun? Astron Lett 37:656–658. https://doi.org/10.1134/S0320010811080031. arXiv:1109.1351 [astro-ph.SR]

Kitchatinov LL, Olemskoy SV (2012) Solar dynamo model with diamagnetic pumping and nonlocal α-effect. Sol Phys 276:3–17. https://doi.org/10.1007/s11207-011-9887-2. arXiv:1108.3138 [astro-ph.SR]

Kitchatinov LL, Olemskoy SV (2016) Dynamo model for grand maxima of solar activity: can superflares occur on the Sun? Mon Not R Astron Soc 459(4):4353–4359. https://doi.org/10.1093/mnras/stw875. arXiv:1602.08840 [astro-ph.SR]

Kitchatinov LL, Rüdiger G (1999) Differential rotation models for late-type dwarfs and giants. Astron Astrophys 344:911–917

Kitchatinov LL, Pipin VV, Rüdiger G (1994a) Turbulent viscosity, magnetic diffusivity, and heat conductivity under the influence of rotation and magnetic field. Astron Nachr 315:157–170. https://doi.org/10.1002/asna.2103150205

Kitchatinov LL, Rüdiger G, Küker M (1994b) Lambda-quenching as the nonlinearity in stellar-turbulence dynamos. Astron Astrophys 292:125–132

Kitchatinov LL, Pipin VV, Makarov VI, Tlatov AG (1999) Solar torsional oscillations and the grand activity cycle. Sol Phys 189(2):227–239. https://doi.org/10.1023/A:1005260008532

Kitchatinov LL, Mordvinov AV, Nepomnyashchikh AA (2018) Modelling variability of solar activity cycles. Astron Astrophys 615:A38. https://doi.org/10.1051/0004-6361/201732549. arXiv:1804.02833 [astro-ph.SR]

Knobloch E, Tobias SM, Weiss NO (1998) Modulation and symmetry changes in stellar dynamos. Mon Not R Astron Soc 297(4):1123–1138. https://doi.org/10.1046/j.1365-8711.1998.01572.x

Krause F, Rädler KH (1980) Mean-field magnetohydrodynamics and dynamo theory. Pergamon Press, Oxford

Kueker M, Rüdiger G, Pipin VV (1996) Solar torsional oscillations due to the magnetic quenching of the Reynolds stress. Astron Astrophys 312:615–623

Küker M, Arlt R, Rüdiger G (1999) The Maunder minimum as due to magnetic Λ-quenching. Astron Astrophys 343:977–982

Kumar R, Jouve L, Nandy D (2019) A 3D kinematic Babcock Leighton solar dynamo model sustained by dynamic magnetic buoyancy and flux transport processes. Astron Astrophys 623:A54. https://doi.org/10.1051/0004-6361/201834705. arXiv:1901.04251 [astro-ph.SR]

Kumar P, Karak BB, Vashishth V (2021) Supercriticality of the dynamo limits the memory of the polar field to one cycle. Astrophys J 913(1):65. https://doi.org/10.3847/1538-4357/abf0a1. arXiv:2103.11754 [astro-ph.SR]

Kumar P, Nagy M, Lemerle A, Karak BB, Petrovay K (2021) The polar precursor method for solar cycle prediction: comparison of predictors and their temporal range. Astrophys J 909(1):87. https://doi.org/10.3847/1538-4357/abdbb4. arXiv:2101.05013 [astro-ph.SR]

Kumar P, Biswas A, Karak BB (2022) Physical link of the polar field buildup with the Waldmeier effect broadens the scope of early solar cycle prediction: Cycle 25 is likely to be slightly stronger than Cycle 24. Mon Not R Astron Soc 513(1):L112–L116. https://doi.org/10.1093/mnrasl/slac043. arXiv:2203.11494 [astro-ph.SR]

Landau LD, Lifshitz EM (1987) Fluid mechanics, course of theoretical physics, vol 6, 2nd edn. Pergamon Press, Oxford

Leighton RB (1964) Transport of magnetic fields on the Sun. Astrophys J 140:1547. https://doi.org/10.1086/148058

Lemerle A, Charbonneau P (2017) A coupled 2 × 2D Babcock–Leighton solar dynamo model. II. Reference dynamo solutions. Astrophys J 834:133. https://doi.org/10.3847/1538-4357/834/2/133. arXiv:1606.07375 [astro-ph.SR]

Lord JW, Cameron RH, Rast MP, Rempel M, Roudier T (2014) The role of subsurface flows in solar surface convection: modeling the spectrum of supergranular and larger scale flows. Astrophys J 793(1):24. https://doi.org/10.1088/0004-637X/793/1/24. arXiv:1407.2209 [astro-ph.SR]

MacGregor KB, Charbonneau P (1997) Solar interface dynamos. I. Linear, kinematic models in Cartesian geometry. Astrophys J 486(1):484–501. https://doi.org/10.1086/304484

Malkus WVR, Proctor MRE (1975) The macrodynamics of alpha-effect dynamos in rotating fluids. J Fluid Mech 67:417–443. https://doi.org/10.1017/S0022112075000390

Mandal S, Karak BB, Banerjee D (2017) Latitude distribution of sunspots: analysis using sunspot data and a dynamo model. Astrophys J 851:70. https://doi.org/10.3847/1538-4357/aa97dc. arXiv:1711.00222 [astro-ph.SR]

Martin-Belda D, Cameron RH (2017) Inflows towards active regions and the modulation of the solar cycle: a parameter study. Astron Astrophys 597:A21. https://doi.org/10.1051/0004-6361/201629061. arXiv:1609.01199 [astro-ph.SR]

McClintock BH, Norton AA, Li J (2014) Re-examining sunspot tilt angle to include anti-Hale statistics. Astrophys J 797:130. https://doi.org/10.1088/0004-637X/797/2/130. arXiv:1412.5094 [astro-ph.SR]

McIntosh SW, Leamon RJ, Gurman JB, Olive JP, Cirtain JW, Hathaway DH, Burkepile J, Miesch M, Markel RS, Sitongia L (2013) Hemispheric asymmetries of solar photospheric magnetism: radiative, particulate, and heliospheric impacts. Astrophys J 765:146. https://doi.org/10.1088/0004-637X/765/2/146. arXiv:1302.1081 [astro-ph.SR]

Metcalfe TS, Egeland R, van Saders J (2016) Stellar evidence that the solar dynamo may be in transition. Astrophys J Lett 826(1):L2. https://doi.org/10.3847/2041-8205/826/1/L2. arXiv:1606.01926 [astro-ph.SR]

Miesch MS, Dikpati M (2014) A three-dimensional Babcock–Leighton solar dynamo model. Astrophys J Lett 785:L8. https://doi.org/10.1088/2041-8205/785/1/L8. arXiv:1401.6557 [astro-ph.SR]

Miesch MS, Teweldebirhan K (2016) A three-dimensional Babcock–Leighton solar dynamo model: initial results with axisymmetric flows. Adv Space Res 58(8):1571–1588. https://doi.org/10.1016/j.asr.2016.02.018. arXiv:1511.03613 [astro-ph.SR]

Miyahara H, Tokanai F, Moriya T, Takeyama M, Sakurai H, Horiuchi K, Hotta H (2021) Gradual onset of the Maunder minimum revealed by high-precision carbon-14 analyses. Sci Rep 11:5482. https://doi.org/10.1038/s41598-021-84830-5

Mordvinov A, Pevtsov A, Bertello L, Petri G (2016) The reversal of the Sun's magnetic field in cycle 24. Solar Terrest Phys 2(1):3–18. https://doi.org/10.12737/16356. arXiv:1602.02460 [astro-ph.SR]

Mordvinov AV, Karak BB, Banerjee D, Chatterjee S, Golubeva EM, Khlystova AI (2020) Long-term evolution of the Sun's magnetic field during Cycles 15–19 based on their proxies from Kodaikanal

Solar Observatory. Astrophys J Lett 902(1):L15. https://doi.org/10.3847/2041-8213/abba80. arXiv:2009.11174 [astro-ph.SR]
Mordvinov AV, Karak BB, Banerjee D, Golubeva EM, Khlystova AI, Zhukova AV, Kumar P (2022) Evolution of the Sun's activity and the poleward transport of remnant magnetic flux in Cycles 21–24. Mon Not R Astron Soc 510(1):1331–1339. https://doi.org/10.1093/mnras/stab3528. arXiv:2111.15585 [astro-ph.SR]
Moss D, Brooke J (2000) Towards a model for the solar dynamo. Mon Not R Astron Soc 315(3):521–533. https://doi.org/10.1046/j.1365-8711.2000.03452.x
Moss D, Sokoloff D, Usoskin I, Tutubalin V (2008) Solar grand minima and random fluctuations in dynamo parameters. Sol Phys 250:221–234
Muñoz-Jaramillo A, Dasi-Espuig M, Balmaceda LA, DeLuca EE (2013) Solar cycle propagation, memory, and prediction: insights from a century of magnetic proxies. Astrophys J Lett 767:L25. https://doi.org/10.1088/2041-8205/767/2/L25. arXiv:1304.3151 [astro-ph.SR]
Muhli P, Brandenburg A, Moss D, Tuominen I (1995) Multiple far-supercritical solutions for an αΛ-dynamo. Astron Astrophys 296:700
Mursula K, Usoskin IG, Kovaltsov GA (2001) Persistent 22-year cycle in sunspot activity: evidence for a relic solar magnetic field. Sol Phys 198(1):51–56. https://doi.org/10.1023/A:1005218414790
Nagy M, Lemerle A, Labonville F, Petrovay K, Charbonneau P (2017) The effect of "rogue" active regions on the solar cycle. Sol Phys 292:167. https://doi.org/10.1007/s11207-017-1194-0. arXiv:1712.02185 [astro-ph.SR]
Nagy M, Lemerle A, Charbonneau P (2020) Impact of nonlinear surface inflows into activity belts on the solar dynamo. J Space Weather Space Clim 10:62. https://doi.org/10.1051/swsc/2020064
Nandy D, Choudhuri AR (2000) The role of magnetic buoyancy in a Babcock–Leighton type solar dynamo. J Astrophys Astron 21:381. https://doi.org/10.1007/BF02702429
Nelson NJ, Brown BP, Brun AS, Miesch MS, Toomre J (2013) Magnetic wreaths and cycles in convective dynamos. Astrophys J 762:73. https://doi.org/10.1088/0004-637X/762/2/73. arXiv:1211.3129 [astro-ph.SR]
Oláh K, Kővári Z, Petrovay K, Soon W, Baliunas S, Kolláth Z, Vida K (2016) Magnetic cycles at different ages of stars. Astron Astrophys 590:A133. https://doi.org/10.1051/0004-6361/201628479. arXiv:1604.06701 [astro-ph.SR]
Ölçek D, Charbonneau P, Lemerle A, Longpré G, Boileau F (2019) Grand activity minima and maxima via dual dynamos. Sol Phys 294(7):99. https://doi.org/10.1007/s11207-019-1492-9
Olemskoy SV, Kitchatinov LL (2013) Grand minima and north–south asymmetry of solar activity. Astrophys J 777:71. https://doi.org/10.1088/0004-637X/777/1/71
Oliveira DN, Rempel EL, Chertovskih R, Karak BB (2021) Chaotic transients and hysteresis in an α^2 dynamo model. J Phys Complex 2(2):025012. https://doi.org/10.1088/2632-072X/abd1c6. arXiv:2012.02064 [physics.plasm-ph]
Ossendrijver AJH, Hoyng P (1996) Stochastic and nonlinear fluctuations in a mean field dynamo. Astron Astrophys 313:959–970
Ossendrijver AJH, Hoyng P, Schmitt D (1996) Stochastic excitation and memory of the solar dynamo. Astron Astrophys 313:938–948
Ossendrijver MAJH (2000) Grand minima in a buoyancy-driven solar dynamo. Astron Astrophys 359:364–372
Ossendrijver M (2003) The solar dynamo. Astron Astrophys Rev 11(4):287–367. https://doi.org/10.1007/s00159-003-0019-3
Parker EN (1955a) Hydromagnetic dynamo models. Astrophys J 122:293. https://doi.org/10.1086/146087
Parker EN (1955b) The formation of sunspots from the solar toroidal field. Astrophys J 121:491. https://doi.org/10.1086/146010
Parker EN (1993) A solar dynamo surface wave at the interface between convection and nonuniform rotation. Astrophys J 408:707. https://doi.org/10.1086/172631
Passos D, Charbonneau P (2014) Characteristics of magnetic solar-like cycles in a 3D MHD simulation of solar convection. Astron Astrophys 568:A113. https://doi.org/10.1051/0004-6361/201423700
Passos D, Charbonneau P, Beaudoin P (2012) An exploration of non-kinematic effects in flux transport dynamos. Sol Phys 279(1):1–22. https://doi.org/10.1007/s11207-012-9971-2
Passos D, Nandy D, Hazra S, Lopes I (2014) A solar dynamo model driven by mean-field alpha and Babcock–Leighton sources: fluctuations, grand-minima-maxima, and hemispheric asymmetry in

sunspot cycles. Astron Astrophys 563:A18. https://doi.org/10.1051/0004-6361/201322635. arXiv:1309.2186 [astro-ph.SR]
Passos D, Miesch M, Guerrero G, Charbonneau P (2017) Meridional circulation dynamics in a cyclic convective dynamo. Astron Astrophys 607:A120. https://doi.org/10.1051/0004-6361/201730568. arXiv:1702.02421 [astro-ph.SR]
Petrovay K (2007) On the possibility of a bimodal solar dynamo. Astron Nachr 328(8):777. https://doi.org/10.1002/asna.200710804. arXiv:0708.2131 [astro-ph]
Petrovay K (2020) Solar cycle prediction. Living Rev Sol Phys 17:2. https://doi.org/10.1007/s41116-020-0022-z. arXiv:1907.02107 [astro-ph.SR]
Petrovay K, Nagy M, Yeates AR (2020) Towards an algebraic method of solar cycle prediction. I. Calculating the ultimate dipole contributions of individual active regions. J Space Weather Space Clim 10:50. https://doi.org/10.1051/swsc/2020050. arXiv:2009.02299 [astro-ph.SR]
Pipin VV (1999) The Gleissberg cycle by a nonlinear $\alpha\Lambda$ dynamo. Astron Astrophys 346:295–302
Pipin VV, Kosovichev AG (2019) On the origin of solar torsional oscillations and extended solar cycle. Astrophys J 887(2):215. https://doi.org/10.3847/1538-4357/ab5952. arXiv:1908.04525 [astro-ph.SR]
Poisson M, Démoulin P, Mandrini CH, López Fuentes MC (2020) Active-region tilt angles from white-light images and magnetograms: the role of magnetic tongues. Astrophys J 894(2):131. https://doi.org/10.3847/1538-4357/ab8944. arXiv:2004.07345 [astro-ph.SR]
Pouquet A, Frisch U, Leorat J (1976) Strong MHD helical turbulence and the nonlinear dynamo effect. J Fluid Mech 77:321–354. https://doi.org/10.1017/S0022112076002140
Priyal M, Banerjee D, Karak BB, Muñoz-Jaramillo A, Ravindra B, Choudhuri AR, Singh J (2014) Polar network index as a magnetic proxy for the solar cycle studies. Astrophys J Lett 793:L4. https://doi.org/10.1088/2041-8205/793/1/L4. arXiv:1407.4944 [astro-ph.SR]
Racine É, Charbonneau P, Ghizaru M, Bouchat A, Smolarkiewicz PK (2011) On the mode of dynamo action in a global large-eddy simulation of solar convection. Astrophys J 735:46. https://doi.org/10.1088/0004-637X/735/1/46
Rajaguru SP, Antia HM (2015) Meridional circulation in the solar convection zone: time-distance helioseismic inferences from four years of HMI/SDO observations. Astrophys J 813:114. https://doi.org/10.1088/0004-637X/813/2/114. arXiv:1510.01843 [astro-ph.SR]
Rempel M (2005) Influence of random fluctuations in the Λ-effect on meridional flow and differential rotation. Astrophys J 631(2):1286–1292. https://doi.org/10.1086/432610. arXiv:astro-ph/0610132 [astro-ph]
Rempel M (2006) Flux-transport dynamos with Lorentz force feedback on differential rotation and meridional flow: saturation mechanism and torsional oscillations. Astrophys J 647(1):662–675. https://doi.org/10.1086/505170. arXiv:astro-ph/0604446 [astro-ph]
Rengarajan TN (1984) Age-rotation relationship for late-type main-sequence stars. Astrophys J Lett 283:L63–L65
Ribes JC, Nesme-Ribes E (1993) The solar sunspot cycle in the Maunder minimum AD1645 to AD1715. Astron Astrophys 276:549
Rüdiger G (1989) Differential rotation and stellar convection. Sun and solar-type stars. Akademie-Verlag, Gordon and Breach, Berlin, New York
Rüdiger G, Kichatinov LL (1993) Alpha-effect and alpha-quenching. Astron Astrophys 269(1–2):581–588
Ruzmaikin AA (1981) The solar cycle as a strange attractor. Commun Astrophys 9:85–93
Schmitt D (1985) Dynamowirkung magnetostrophischer Wellen. PhD thesis, University of Göttingen
Schmitt D, Schüssler M (1989) Non-linear dynamos. I. One-dimensional model of a thin layer dynamo. Astron Astrophys 223(1–2):343–351
Schmitt D, Schüssler M, Ferriz-Mas A (1996) Intermittent solar activity by an on–off dynamo. Astron Astrophys 311:L1–L4
Schüssler M (1981) The solar torsional oscillation and dynamo models of the solar cycle. Astron Astrophys 94(2):L17
Schüssler M, Cameron RH (2018) Origin of the hemispheric asymmetry of solar activity. Astron Astrophys 618:A89. https://doi.org/10.1051/0004-6361/201833532. arXiv:1807.10061 [astro-ph.SR]
Senthamizh Pavai V, Arlt R, Dasi-Espuig M, Krivova NA, Solanki SK (2015) Sunspot areas and tilt angles for solar cycles 7–10. Astron Astrophys 584:A73. https://doi.org/10.1051/0004-6361/201527080. arXiv:1508.07849 [astro-ph.SR]
Shah SP, Wright JT, Isaacson H, Howard AW, Curtis JL (2018) HD 4915: a Maunder minimum candidate. Astrophys J Lett 863(2):L26. https://doi.org/10.3847/2041-8213/aad40c. arXiv:1801.09650 [astro-ph.SR]

Simard C, Charbonneau P, Dubé C (2016) Characterisation of the turbulent electromotive force and its magnetically-mediated quenching in a global EULAG-MHD simulation of solar convection. Adv Space Res 58(8):1522–1537. https://doi.org/10.1016/j.asr.2016.03.041. arXiv:1604.01533 [astro-ph.SR]

Solanki SK, Usoskin IG, Kromer B, Schüssler M, Beer J (2004) Unusual activity of the Sun during recent decades compared to the previous 11,000 years. Nature 431:1084–1087. https://doi.org/10.1038/nature02995

Solanki SK, Wenzler T, Schmitt D (2008) Moments of the latitudinal dependence of the sunspot cycle: a new diagnostic of dynamo models. Astron Astrophys 483:623–632. https://doi.org/10.1051/0004-6361:20054282

Solanki SK, Krivova NA, Haigh JD (2013) Solar irradiance variability and climate. Annu Rev Astron Astrophys 51(1):311–351. https://doi.org/10.1146/annurev-astro-082812-141007. arXiv:1306.2770 [astro-ph.SR]

Spiegel EA (1977) Photoconvection. In: Spiegel EA, Zahn JP (eds) Problems of stellar convection. Lecture Notes in Physics, vol 71. Springer, Berlin, pp 267–283. https://doi.org/10.1007/3-540-08532-7_50

Spruit HC (2003) Origin of the torsional oscillation pattern of solar rotation. Sol Phys 213(1):1–21. https://doi.org/10.1023/A:1023202605379. arXiv:astro-ph/0209146 [astro-ph]

Sraibman L, Minotti F (2019) Large-scale model of the axisymmetric dynamo with feedback effects. Sol Phys 294(1):14. https://doi.org/10.1007/s11207-018-1350-1

Sreedevi A, Jha BK, Karak BB, Banerjee D (2023) AutoTAB: automatic tracking algorithm for bipolar magnetic regions. arXiv e-prints https://doi.org/10.48550/arXiv.2304.06615. arXiv:2304.06615 [astro-ph.SR]

Steenbeck M, Krause F, Rädler KH (1966) Berechnung der mittleren Lorentz–Feldstärke für ein elektrisch leitendes Medium in turbulenter, durch Coriolis-Kräfte beeinflußter Bewegung. Z Naturforsch A 21:369. https://doi.org/10.1515/zna-1966-0401

Stenflo JO, Kosovichev AG (2012) Bipolar magnetic regions on the Sun: global analysis of the SOHO/MDI data set. Astrophys J 745:129. https://doi.org/10.1088/0004-637X/745/2/129. arXiv:1112.5226 [astro-ph.SR]

Stix M (2002) The Sun: An Introduction. Springer, Berlin. https://doi.org/10.1007/978-3-642-56042-2

Subramanian K, Brandenburg A (2004) Nonlinear current helicity fluxes in turbulent dynamos and alpha quenching. Phys Rev Lett 93(20):205001. https://doi.org/10.1103/PhysRevLett.93.205001. arXiv:astro-ph/0408020 [astro-ph]

Suess HE (1980) The radiocarbon record in tree rings of the last 8000 years. Radiocarbon 22:200–209. https://doi.org/10.1017/S0033822200009462

Talafha M, Nagy M, Lemerle A, Petrovay K (2022) Role of observable nonlinearities in solar cycle modulation. Astron Astrophys 660:A92. https://doi.org/10.1051/0004-6361/202142572. arXiv:2112.14465 [astro-ph.SR]

Tavakol RK (1978) Is the Sun almost-intransitive? Nature 276:802. https://doi.org/10.1038/276802a0

Temmer M (2021) Space weather: the solar perspective. Living Rev Sol Phys 18:4. https://doi.org/10.1007/s41116-021-00030-3. arXiv:2104.04261 [astro-ph.SR]

Thelen JC (2000) Non-linear $\alpha\omega$-dynamos driven by magnetic buoyancy. Mon Not R Astron Soc 315(1):165–183. https://doi.org/10.1046/j.1365-8711.2000.03420.x

Tlatov AG (2013) Reversals of Gnevyshev–Ohl rule. Astrophys J Lett 772(2):L30. https://doi.org/10.1088/2041-8205/772/2/L30. arXiv:1304.2518 [astro-ph.SR]

Tlatov A, Illarionov E, Sokoloff D, Pipin V (2013) A new dynamo pattern revealed by the tilt angle of bipolar sunspot groups. Mon Not R Astron Soc 432(4):2975–2984. https://doi.org/10.1093/mnras/stt659. arXiv:1302.2715 [astro-ph.SR]

Tobias SM (1997) The solar cycle: parity interactions and amplitude modulation. Astron Astrophys 322:1007–1017

Tripathi B, Nandy D, Banerjee S (2021) Stellar mid-life crisis: subcritical magnetic dynamos of solar-like stars and the breakdown of gyrochronology. Mon Not R Astron Soc 506(1):L50–L54. https://doi.org/10.1093/mnrasl/slab035. arXiv:1812.05533 [astro-ph.SR]

Upton L, Hathaway DH (2014a) Effects of meridional flow variations on solar Cycles 23 and 24. Astrophys J 792(2):142. https://doi.org/10.1088/0004-637X/792/2/142. arXiv:1408.0035 [astro-ph.SR]

Upton L, Hathaway DH (2014b) Predicting the Sun's polar magnetic fields with a surface flux transport model. Astrophys J 780(1):5. https://doi.org/10.1088/0004-637X/780/1/5. arXiv:1311.0844 [astro-ph.SR]

Usoskin IG (2023) A history of solar activity over millennia. Living Rev Sol Phys 20:2. https://doi.org/10.1007/s41116-023-00036-z
Usoskin IG, Mursula K, Kovaltsov GA (2000) Cyclic behaviour of sunspot activity during the Maunder minimum. Astron Astrophys 354:L33–L36
Usoskin IG, Solanki SK, Kovaltsov GA (2007) Grand minima and maxima of solar activity: new observational constraints. Astron Astrophys 471:301–309
Usoskin IG, Hulot G, Gallet Y, Roth R, Licht A, Joos F, Kovaltsov GA, Thébault E, Khokhlov A (2014) Evidence for distinct modes of solar activity. Astron Astrophys 562:L10
Usoskin IG, Arlt R, Asvestari E, Hawkins E, Käpylä M, Kovaltsov GA, Krivova N, Lockwood M, Mursula K, O'Reilly J, Owens M, Scott CJ, Sokoloff DD, Solanki SK, Soon W, Vaquero JM (2015) The Maunder minimum (1645–1715) was indeed a grand minimum: a reassessment of multiple datasets. Astron Astrophys 581:A95. https://doi.org/10.1051/0004-6361/201526652. arXiv:1507.05191 [astro-ph.SR]
Usoskin IG, Solanki SK, Krivova NA, Hofer B, Kovaltsov GA, Wacker L, Brehm N, Kromer B (2021) Solar cyclic activity over the last millennium reconstructed from annual ^{14}C data. Astron Astrophys 649:A141. https://doi.org/10.1051/0004-6361/202140711. arXiv:2103.15112 [astro-ph.SR]
Vaquero JM, Gallego MC, Usoskin IG, Kovaltsov GA (2011) Revisited sunspot data: a new scenario for the onset of the Maunder minimum. Astrophys J Lett 731(2):L24. https://doi.org/10.1088/2041-8205/731/2/L24. arXiv:1103.1520 [astro-ph.SR]
Vaquero JM, Kovaltsov GA, Usoskin IG, Carrasco VMS, Gallego MC (2015) Level and length of cyclic solar activity during the Maunder minimum as deduced from the active-day statistics. Astron Astrophys 577:A71. https://doi.org/10.1051/0004-6361/201525962. arXiv:1503.07664 [astro-ph.SR]
Vashishth V (2022) Modelling the occurrence of grand minima in Sun-like stars using a dynamo model. arXiv e-prints https://doi.org/10.48550/arXiv.2212.01795. arXiv:2212.01795 [astro-ph.SR]
Vashishth V, Karak BB, Kitchatinov L (2021) Subcritical dynamo and hysteresis in a Babcock–Leighton type kinematic dynamo model. Res Astron Astrophys 21(10):266. https://doi.org/10.1088/1674-4527/21/10/266. arXiv:2107.01546 [astro-ph.SR]
Vashishth V, Karak BB, Kitchatinov L (2023) Dynamo modelling for cycle variability and occurrence of grand minima in Sun-like stars: rotation rate dependence. Mon Not R Astron Soc 522(2):2601–2610. https://doi.org/10.1093/mnras/stad1105. arXiv:2304.05819 [astro-ph.SR]
Viviani M, Warnecke J, Käpylä MJ, Käpylä PJ, Olspert N, Cole-Kodikara EM, Lehtinen JJ, Brandenburg A (2018) Transition from axi- to non-axisymmetric dynamo modes in spherical convection models of solar-like stars. Astron Astrophys 616:A160. https://doi.org/10.1051/0004-6361/201732191. arXiv:1710.10222 [astro-ph.SR]
Viviani M, Käpylä MJ, Warnecke J, Käpylä PJ, Rheinhardt M (2019) Stellar dynamos in the transition regime: multiple dynamo modes and antisolar differential rotation. Astrophys J 886(1):21. https://doi.org/10.3847/1538-4357/ab3e07. arXiv:1902.04019 [astro-ph.SR]
Waldmeier M (1955) Ergebnisse und Probleme der Sonnenforschung. Geest & Portig, Leipzig
Wang YM, Sheeley NR (2009) Understanding the geomagnetic precursor of the solar cycle. Astrophys J Lett 694:L11–L15. https://doi.org/10.1088/0004-637X/694/1/L11
Wang YM, Nash AG, Sheeley JNR (1989) Magnetic flux transport on the Sun. Science 245(4919):712–718. https://doi.org/10.1126/science.245.4919.712
Wang YM, Sheeley NR Jr, Nash AG (1991) A new solar cycle model including meridional circulation. Astrophys J 383:431–442. https://doi.org/10.1086/170800
Wang YM, Colaninno RC, Baranyi T, Li J (2015) Active-region tilt angles: magnetic versus white-light determinations of Joy's law. Astrophys J 798(1):50. https://doi.org/10.1088/0004-637X/798/1/50. arXiv:1412.2329 [astro-ph.SR]
Warnecke J, Rheinhardt M, Tuomisto S, Käpylä PJ, Käpylä MJ, Brandenburg A (2018) Turbulent transport coefficients in spherical wedge dynamo simulations of solar-like stars. Astron Astrophys 609:A51. https://doi.org/10.1051/0004-6361/201628136. arXiv:1601.03730 [astro-ph.SR]
Weiss NO, Tobias SM (2016) Supermodulation of the Sun's magnetic activity: the effects of symmetry changes. Mon Not R Astron Soc 456(3):2654–2661. https://doi.org/10.1093/mnras/stv2769
Weiss NO, Cattaneo F, Jones CA (1984) Periodic and aperiodic dynamo waves. Geophys Astrophys Fluid Dyn 30:305–341. https://doi.org/10.1080/03091928408219262
Wilmot-Smith AL, Nandy D, Hornig G, Martens PCH (2006) A time delay model for solar and stellar dynamos. Astrophys J 652(1):696–708. https://doi.org/10.1086/508013

Wu CJ, Usoskin IG, Krivova N, Kovaltsov GA, Baroni M, Bard E, Solanki SK (2018) Solar activity over nine millennia: a consistent multi-proxy reconstruction. Astron Astrophys 615:A93. https://doi.org/10.1051/0004-6361/201731892. arXiv:1804.01302 [astro-ph.SR]

Yeates AR, Muñoz-Jaramillo A (2013) Kinematic active region formation in a three-dimensional solar dynamo model. Mon Not R Astron Soc 436(4):3366–3379. https://doi.org/10.1093/mnras/stt1818. arXiv:1309.6342 [astro-ph.SR]

Yeates AR, Nandy D, Mackay DH (2008) Exploring the physical basis of solar cycle predictions: flux transport dynamics and persistence of memory in advection- versus diffusion-dominated solar convection zones. Astrophys J 673:544–556. https://doi.org/10.1086/524352. arXiv:0709.1046

Yoshimura H (1975) Solar-cycle dynamo wave propagation. Astrophys J 201:740–748. https://doi.org/10.1086/153940

Yoshimura H (1978) Nonlinear astrophysical dynamos: multiple-period dynamo wave oscillations and long-term modulations of the 22 year solar cycle. Astrophys J 226:706–719. https://doi.org/10.1086/156653

Zolotova NV, Ponyavin DI (2015a) The Gnevyshev–Ohl rule and its violations. Geomag Aeron 55(7):902–906. https://doi.org/10.1134/S0016793215070300

Zolotova NV, Ponyavin DI (2015b) The Maunder minimum is not as grand as it seemed to be. Astrophys J 800(1):42. https://doi.org/10.1088/0004-637x/800/1/42

Zolotova NV, Ponyavin DI (2016) How deep was the Maunder minimum? Sol Phys 291:2869–2890. https://doi.org/10.1007/s11207-016-0908-z